הטכניון - מכון טכנולוגי לישראל
הפקולטה להנדסת אוירונוטיקה וחלל

TECHNION-Israel Institute of Technology
Faculty of Aerospace Engineering

ADVANCED INTERACTIVE DISPLAY FORMATS FOR TERMINAL AREA TRAFFIC CONTROL

A Joint Research Project Between NASA Ames Research Center, Moffett Field, Ca, and The Faculty of Aerospace Engineering at the Technion, Israel Institute Of Technology, Haifa, Israel

Final Report and Proposal for Continued Research

Cooperative Grant No.: NCCW-0045

Arthur J. Grunwald
Faculty of Aerospace Engineering
Technion, Israel Institute of Technology
Haifa, 32000, ISRAEL

January 8, 1996

ADVANCED INTERACTIVE DISPLAY FORMATS FOR TERMINAL AREA TRAFFIC CONTROL

A Joint Research Project Between NASA Ames Research Center, Moffett Field, Ca, and The Faculty of Aerospace Engineering at the Technion, Israel Institute Of Technology, Haifa, Israel

Final report for the period: October 1, 1994 - Sept. 30, 1995;

Proposal for continued research for the period: Jan. 1, 1996 - Dec. 31, 1996[1]

Cooperative Grant No.: NCCW-0045

Principal Investigator:

Associate Professor Arthur J. Grunwald
Faculty of Aerospace Engineering
Technion, Israel Institute of Technology
Haifa, 32000, ISRAEL

Contract Technical Monitor:

Dr. Stephen R. Ellis
Mail Stop 262-2
NASA Ames Research Center
Moffett Field, CA. 94035
USA

PREFACE

This report describes a continuing cooperative research effort between NASA Ames Research Center and the Faculty of Aerospace Engineering, Technion, Haifa, Israel, in the area of advanced pictorial displays for aerospace applications. The efforts will be focused on the development of advanced display formats for Center-TRACON Air Traffic Control displays. This final report describes the basic principles and software developments for manual viewing parameter setting in perspective Air Traffic Control Displays. Chapter 6 of this report contains an outline of the proposed activities for continued research. The proposed, continued research efforts will, among others, deal with automated viewing parameter setting according to a well-chosen optimization strategy.

---

[1]The period Oct. 1, 1995-Dec. 31, 1995 is considered as an extension without additional costs. The time was used for reporting and outlining the continued reserach.

ABSTRACT

This report describes the basic design considerations for perspective Air Traffic Control displays. A software framework has been developed for manual viewing parameter setting (MVPS) in preparation for continued, ongoing developments on automated viewing parameter setting (AVPS) schemes. Two distinct modes of MVPS operations are considered, both of which utilize manipulation pointers imbedded in the three-dimensional scene: (1) *direct* manipulation of the viewing parameters; in this mode the manipulation pointers act like the control-input device, through which the viewing parameter changes are made. Part of the parameters are rate controlled, and part of them position controlled. This mode is intended for making fast, iterative small changes in the parameters. (2) *indirect* manipulation of the viewing parameters. This mode is intended primarily for introducing large, predetermined changes in the parameters. Requests for changes in viewing parameter setting are entered manually by the operator by moving viewing parameter manipulation pointers on the screen. The motion of these pointers, which are an integral part of the 3-D scene, is limited to the boundaries of screen. This arrangement has been chosen, in order to preserve the correspondence between the spatial lay-outs of the new and the old viewing parameter setting, a feature which contributes to preventing spatial disorientation of the operator. For all viewing operations, e.g. rotation, translation and ranging, the actual change is executed automatically by the system, through gradual transitions with an exponentially damped, sinusoidal velocity profile, in this work referred to as 'slewing' motions. The slewing functions, which eliminate discontinuities in the viewing parameter changes, are designed primarily for enhancing the operator's impression that he, or she, is dealing with an actually existing physical system, rather than an abstract computer-generated scene. The proposed, continued research efforts will deal with the development of automated viewing parameter setting schemes. These schemes employ an optimization strategy, aimed at identifying the best possible vantage point, from which the Air Traffic Control scene can be viewed for a given traffic situation. They determine whether a change in viewing parameter setting is required and determine the dynamic path along which the change to the new viewing parameter setting should take place.

TABLE OF CONTENTS

ABSTRACT i

TABLE OF CONTENTS ii

LIST OF FIGURES iv

LIST OF TABLES iv

CHAPTER 1.: BACKGROUND 1

1.1. Focus of Interest of this Research 1
1.2. 'Conventional' Plan View Displays vs. Perspective Displays 1
1.2. The Purpose of the Research 2

CHAPTER 2.: BASIC DESIGN CONSIDERATIONS 3

2.1. Definition of Coordinate Systems 4
2.2. Basic Viewing Parameters 4
2.3. Constraint Viewing Operations 4
2.4. Direct vs. Indirect Manipulation 6
2.5. Enlargement of Vertical Scaling 6
2.6. One-Control button Operation With 2-D Analog Device 7

CHAPTER 3.: VIEWING PARAMETER OPERATIONS 8

3.1. Viewing Parameter Changes Through Slewing Motions 8
3.2. Mathematical Formulation 8
3.3. Time Histories of Slewing Functions 10
3.4. Determination of Slewing Parameter Values 11
3.4.1. Determination of the slewing time 11
3.4.2. Determination of the damping coefficient 11
3.5. Manipulation Pointers 13
3.6. Sequence of Operations 13
3.6.1. Choosing the operation by selecting the appropriate pointer 13
3.6.2. Positioning the pointer 14
3.6.3. Enhancement of the screen cursor 14
3.6.4. Executing the requested change 14

CHAPTER 4.: DESCRIPTION OF DISPLAY 15

4.1. Selection of Objects 15
4.2. Menus and Menu Operations 15
4.3. Manual Viewing Parameter Setting (MVPS) Operations 18
4.3.1. Translate mode 18
4.3.2. Rotate mode 27
4.3.3. Range mode 28
4.3.4. Reset and return options 29

TABLE OF CONTENTS (CONTINUED)

CHAPTER 5.: AUTOMATED VIEWING PARAMETER SETTING 30

5.1. Automated Viewing Parameter Setting (AVPS) 30
5.2. Design Requirements for AVPS Operations 31
5.3. Principle of Operation of the AVPS 32
5.4. Estimation of the Relative Spatial Position Between Aircraft 32
5.4.1. Geometry of the 3-D situation 32
5.4.2. Cost associated with estimation errors 34
5.5. Computation of the Global Cost 36
5.6. Impact of Individual Aircraft on the Global Cost 36
5.7. Optimization Method 37

CHAPTER 6.: PROPOSED CONTINUED RESEARCH 38

6.1. Current Status of the Research 38
6.2. Analytical and System Developments 38
6.2.1. Enhanced visual perception modeling 38
6.2.2. Enhanced noise modeling for multi-object scenes 43
6.2.3. Parametric study of the enhanced noise model 44
6.2.4. AVPS system development 46
6.2.5. Analytical tests of the AVPS system 47
6.2.6. Decision algorithm 47
6.2.7. Path-planning algorithm 47
6.3. Experimental Evaluations 49
6.3.1. Experimental validation of the enhanced noise model 49
6.3.2. AVPS Operator-in-the-loop experiments 49
6.3.3. Experimental evaluation of slewing functions 50
6.4. Summary of Proposed Activities Jan. 1, 1996 - Dec. 31, 1996 51
6.5. Estimated Budged for the Period Jan. 1, 1996 - Dec. 31 19967 52

LIST OF FIGURES

Figure 1.: Viewing situation geometry 3
Figure 2.: Concept of enlargement of vertical scaling 6
Figure 3.: Time histories of slew function and slew rate for $\zeta = 0.6$ 9
Figure 4.: Direct and indirect modes for manipulation pointers 12
Figure 5.: General screen image in the viewing mode 16
Figure 6a.: Manipulation pointers for indirect translate operations 17
Figure 6b.: Manipulation pointers for direct translate operations 19
Figure 7.: Digital position read-out in the translate mode 20
Figure 8a.: Manipulation pointers for the rotate mode; pitch operations 21
Figure 8b.: Manipulation pointers for the rotate mode; yaw operations 22
Figure 9a.: Manipulation pointers for indirect ranging operations 23
Figure 9b.: Manipulation pointers for direct ranging operations; ranging out 24
Figure 9c.: Manipulation pointers for direct ranging operations; ranging in 25
Figure 10.: Geometry of ranging operation 26
Figure 11.: Perspective view of two spatially separated aircraft 31
Figure 12.: The effect of line-of-sight noise on spatial estimates 33
Figure 13.: Shape distortions for constant-magnitude and correlated LOS noise 39
Figure 14.: LOS noise component, correlated with neighboring vertices 40
Figure 15.: Perceived object shape distortion 41
Figure 16.: Noise component, set by inter-object relations 42
Figure 17.: Spatial orientation of trapezoid with respect to LOS to point A' 45
Figure 18.: Enhanced LOS noise model validation; the response trapezoid 48

LIST OF TABLES

Table 1.: Time table of proposed activities Jan. 1, 1996 - Dec. 31, 1996 51

1

BACKGROUND

1.1. Focus of Interest of this Research

Increasing the Terminal Area Productivity involves increasing the number of aircraft in the terminal area, decreasing the minimal separation distance between aircraft and minimizing the delays. This might involve the use of complex, curved approach trajectories with a build-in flexibility to introduce fast, dynamic changes, where all operations in this environment are subject to stringent safety requirements.

The increased productivity will also involve increased interaction with each one of the aircraft in the area, and consequently, will result in increased task complexity of the Air Traffic Controller. Although automated sequencing, scheduling and route generation optimization tools are vital attributes in this complex environment, this research is focused on the Human Controller Interface. This interface must allow the controller to monitor, manage and control this complex environment through effective interaction with the automated system.

1.2. 'Conventional' Plan View Displays vs. Perspective Displays

Air Traffic Control Displays conventionally represent a plan view of the Air Traffic area. The advantage of this approach is that the interpretation of the ground-track aircraft positions is straight-forward and all viewed areas in the arena are 'weighted' with equal importance. On the other hand, perspective displays present the view of a 3-D scene from a well chosen vantage point, and thus integrate the horizontal situation with altitude separation by visualizing the 4-D (Spatial position + velocity) trajectories and constraints in one perspective format. Thus perspective displays offer the advantage that the altitudes of the aircraft, which in the conventional format were represented by data tags, are inherently present in the perspective scene. Thus, two aircraft with nearby ground-track positions, but separated in altitude, will appear 'clustered' on the plan view display, but will appear clearly separated on the perspective display.

In addition to this advantage, the third dimension in perspective displays offer the option of more easy and effective three-dimensional routing, for example, in situations where an upcoming weather front demands re-routing of the traffic flow, or when due to exceptional back-up or emergencies a feeder gate is being closed.

However, perspective Air Traffic Control displays under certain conditions, might have possible disadvantages. These disadvantages are: (1) fast and/or badly designed viewing parameters operations might lead to disorientation of the operator, or impair the operator's spatial awareness, which is a vital attribute in Air Traffic Control tasks; (2) the estimation of relative orientation between objects in the three-dimensional field from perspective views, might be subject to inherent systematic errors, as shown in earlier work[2] ; (3) an incorrectly chosen viewpoint might result in clutter, exclusion of aircraft symbols from the view, or ambiguities in determining spatial positions; (4) the perspective view inherently biases the allocation of attention to nearby, centrally viewed areas, on the account of far-away areas in the periphery; (5) perspective displays, based on single-width, single intensity monochrome wire-frame graphics, might have ambiguities in their spatial representation, e.g. the 'Necker' cube effect, or the well-known 'inverse depth cueing' effects due to clustering of lines at far-away distances.

In order to be able to utilize the full potential of perspective displays and to avoid the above mentioned possible disadvantages, effective and well-designed viewing parameter manipulations are essential. Carefully controlled and well chosen viewing parameters can eliminate the potential disadvantages (1) to (3), whereas automated, optimizing viewing parameter setting schemes might direct the operator's attention to critical areas, thus turning disadvantage (4) into an advantage. However, the effectiveness of viewing parameter settings directed by automated schemes, will largely depend on the dynamic path along which the change to the new viewing parameter setting is to take place. Furthermore, up-to-date real-time computer graphics technology such as solid modeling, texture mapping, shading and alpha blending (realizing semi-transparent surfaces) are able to generate impressively realistic scenes with sufficient update rate, which almost entirely eliminate disadvantage (5).

1.2. The Purpose of the Research

The purpose of the research is to find the basic rules and techniques for utilizing the full potential of *perspective* displays for Air Traffic Control. The display should allow manual and computer-aided traffic flow management and 4-D path planning. The display should enable the operator a clear and unambiguous assessment of the 3-D traffic situation. An essential aspect of the problem is the development of manual and automated viewing parameter manipulations, which enable to utilize the 3-D potential of the perspective display to the full extent, while avoiding the possible disadvantages. In this final report the basic principles and software developments for manual viewing parameter setting in perspective Air Traffic Control Displays are described, and methods for automated viewing parameter setting, are proposed in the framework of continued research.

---

[2] Grunwald, A.J., Ellis, S.R. and Smith, S., "A Mathematical Model for Spatial Orientation from Pictorial Perspective Displays," IEEE Trans. on SMC, Vol. 18, No. 3, May, June 1988, pp. 425-437.

2

BASIC DESIGN CONSIDERATIONS

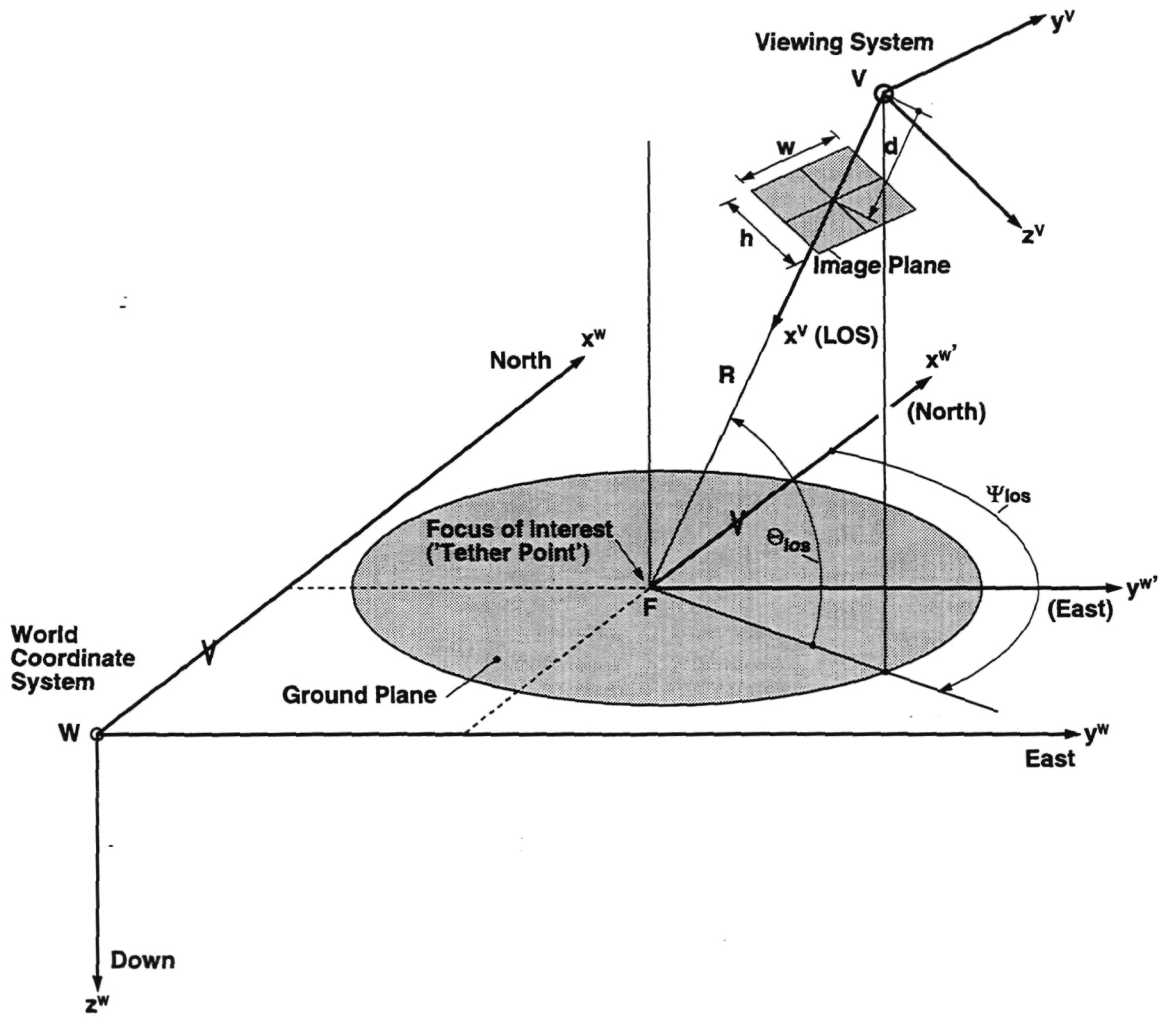

Figure 1.: Viewing situation geometry

2.1. Definition of Coordinate Systems

The Air traffic Control scene is described in a world coordinate system W, with the x^W-axis pointing to the north, the y^W-axis to the east and the z^W-axis downwards. The origin of this system, W, is placed at a fixed reference location, such as an ILS/VOR station at the central airport. For low-altitude displays, the 3-D terrain features, like mountains, obstacles, etc., should be modeled as well. For high-altitude displays, the 3-D terrain features are less important and the terrain can be modeled as a 'flat' texture map.

A viewing system V is defined with the viewer's eye point at the origin and the x^V-axis being the line-of-sight, or viewing axis. The y^V- and z^V-axes are pointing to the right and downwards, respectively, see Fig. 1. The perspective scene is projected on an image plane in front of the viewer. The height h and width w, and distance of this image plane from the viewer's eye, d, determine the horizontal and vertical field-of-view. In this case, the image plane is the monitor screen. For correct viewing, the eye should be positioned at the viewing system's origin V (the 'station point'). However, for the usual dimensions of the monitor screen and the average distance from which the screen is viewed, the field-of-view angles might not be large enough for sufficient coverage of the scene. In this case, the station point will be chosen closer to the screen than the actual eye position.

2.2. Basic Viewing Parameters

The viewing parameters include the $x^W y^W z^W$ coordinates of the viewing system origin V in the world coordinate system W, the yaw, pitch and roll Euler angles, ψ, θ, ϕ, which determine the angular orientation of the viewing system V with respect to the world coordinate system W, the dimensions of the image plane h and w, and the distance d of the image plane from the viewer's eye. The dimensions of the image plane are determined by the dimensions of the screen (in the case the full screen area is used), or the dimensions of a viewport (in the case only part of the screen is used). The distance d determines the zoom-angle or field-of-view. The three spatial coordinates of the viewing system origin V, the three angles determining its angular orientation in space, and the distance d yields 7 independent viewing parameters. Since control over each one of these 7 viewing parameters is impractical, it is necessary to constrain the viewing operations to predetermined patterns.

2.3. Constraint Viewing Operations

The pattern, chosen for the Air Traffic Control scene, is the 'tethered' viewpoint control, shown in Fig. 1. A 'focus-of-interest' is defined in the ground plane. By 'tethering' the viewpoint V around this point, the viewing axis, or Line-of-Sight (LOS), remains at all times directed towards the focus-of-interest. Furthermore, by choosing both the base of the image plane and the y^V axis to be parallel to the ground plane, the roll-angle ϕ will remain zero, and the horizon will appear at all times as a horizontal line on the display.

The tethered viewing parameter setting is accomplished by three independent operations: (1) *translation* of the focus-of-interest in the ground plane; (2) *rotation* of the viewing axis by the azimuth angle[3] Ψ_{los} and the elevation angle Θ_{los}; (3) *ranging*, which is the displacement of the viewpoint along the viewing axis.

The ranging operation will allow areas of interest to be studied from close-by. This operation resembles a 'zooming' operation of a camera, in the sense that, in both cases, areas of interest are enlarged. The basic difference, however, is that a zooming operation is achieved by changing the distance d of the image plane from the viewer's eye, while keeping the screen dimensions and the viewing range the same.

Since for large zoom angles and a flat image plane, the image will appear distorted, a ranging operation, rather than a zooming operation has been chosen. Consequently, a fixed value of d was used, so that viewing operations involve a total of only 5 viewing parameters to be set.

2.4. Direct vs. Indirect Manipulation

Two distinct modes of viewing parameter manipulation were employed. The first one is a *direct* mode, in which the values of the viewing parameters are directly linked to the control manipulator. Simple proportional control laws are chosen, realizing either pure gain control or rate control. This mode of operation is similar to 'flying an aircraft', with the difference that the motions do not result from aerodynamic forces and moments, but are predetermined by the tethered motion pattern. This mode of operation is useful in particular either when fast, rapid iterative changes are required, or when a constant rate is desired, like a constant turn rate. The second mode is the *indirect* mode. In this mode, the operator first introduces a request for a change in one of the viewing parameters. After this request has been entered, the actual change is made automatically by the system, through a smooth and controlled gradual transition from one viewing parameter setting to the new one, in this work referred to as a 'slewing motion'. This mode is useful when relatively large changes are requested from the system. After entering the requested change, the operator is 'unburdened' from executing the actual change. In the AVPS mode the requested change might originate from an optimization scheme. Since both MVPS and AVPS use the same manipulation pointers, the indirect mode allows natural and easy switching between automated and manual viewing parameter setting.

2.5. Enlargement of Vertical Scaling

Enlarged vertical scaling is commonly used in relief maps, with the purpose of enhancing the 3-D features of the terrain. The amount of 'exaggeration' usually depends on the features which the map designer would like to emphasize. In the perspective Air Traffic Control display, the enlargement in vertical scaling should be chosen in accordance with the smallest scale, which still allows a relevant minimal vertical separation distance to be detected by the operator. However, for high-altitude displays this enlarged scaling might result in the ground plane being out of the visible range. In this case it might be necessary to 'center' the enlargement about a given fixed reference height, h_0, different from zero.

---

[3]Note that the azimuth angle of the actual viewing direction is: $\Psi_{los} + 180^0$.

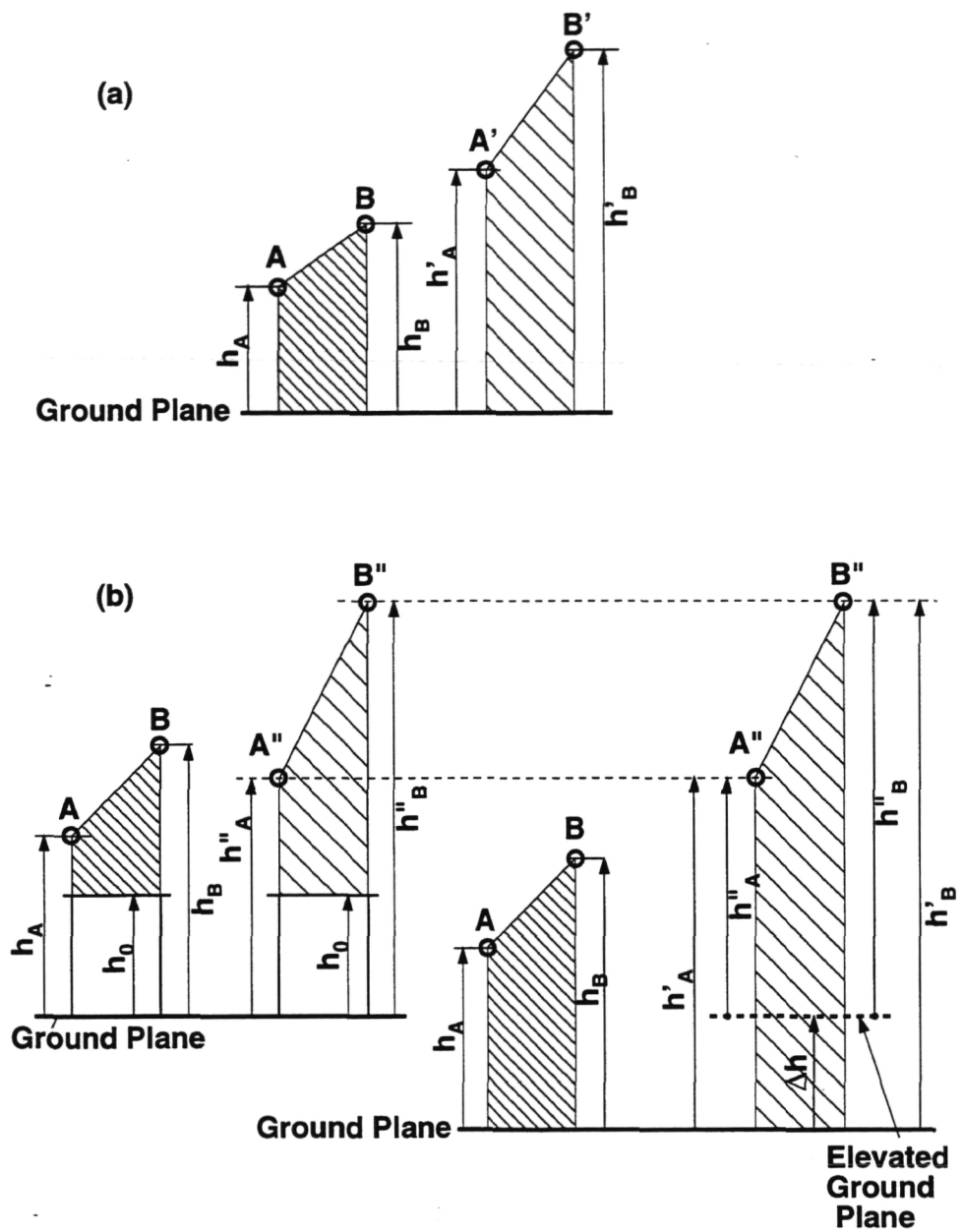

Figure 2.: Concept of enlargement of vertical scaling; (a) enlargement centered at height zero; (b) enlargement centered at height h_0

This concept is demonstrated in Fig. 2. Fig. 2a shows an enlargement of the vertical scale by the factor f, which is centered at the ground plane. After the enlargement, aircraft A and B will be at A' and B', respectively. The 'new' heights are given by:

$$h'_A = fh_A$$
$$h'_B = fh_B \tag{1}$$

However, the new heights h'_A and h'_B might be so large, that the ground plane is no longer within the visible range. In Fig. 2b the enlargement is centered at height h_0. It is clear from this figure that the heights are now:

$$h''_A = f(h_A - h_0) + h_0 = h'_A - (f-1)h_0$$
$$h''_B = f(h_B - h_0) + h_0 = h'_B - (f-1)h_0 \tag{2}$$

The second method is equivalent to a ground plane-centered enlargement of the vertical scaling by the factor f, while at the same time raising the ground plane by the amount:

$$\Delta h = (f-1)h_0 \tag{3}$$

The factor f should be chosen in accordance with the demands for detecting minimal separations, whereas the height h_0 should be chosen such, that the ground plane will be within the visible range. It is clear that in the presence of 3-D terrain features in low-altitude displays, the parameter h_0 must be chosen zero. In all cases f *and* h_0 should be kept fixed during operations.

2.6. One-Control button Operation With 2-D Analog Device

In order to minimize the number of controls and to simplify system operations, all operations are performed with a standard 2-D analog device, with only one active button. Rather than using a multitude of control buttons, the screen cursor is used to select and activate the various attributes on the screen. The options are context sensitive, which means that the appearance of the relevant screen attributes and the control over these attributes, is restricted to the mode of operation the system resides in. This simplifies the selection and eliminates the need for multiple control buttons. In this case a three-button mouse is used as input device. Only the right mouse button is active. The term 'mouse button' as used hereafter, refers to the right mouse button.

Analog control devices are limited to a single 2-D mouse or tracking ball input device. The 2-D control inputs are slaved to the motions of a 2-D screen cursor, where the control gearing is chosen to be fixed. When in an active mode, the screen cursor is visible at all times and its motions are unconstrained. The screen cursor is used to relocate manipulation pointers, which, for example, introduce viewing parameter changes, in 3-D space. However, in contrast to the screen cursor, the motions of these pointers are constrained to their allowed degrees-of-freedom.

3

VIEWING PARAMETER OPERATIONS

3.1. Viewing Parameter Changes Through Slewing Motions

Since discontinuities in the setting of viewing parameters do impair the operator's ability for spatial orientation, all viewing parameter changes are made by means of gradual transitions, which are continuous in rate and acceleration. The time functions, which enable these gradual and smooth transitions are hereafter referred to as 'slewing functions'. Although the term 'slewing' is generally used for pivoting motion, like the rotation of a camera, in this report this term is used for all operations, e.g. rotation, translation and ranging.

3.2. Mathematical Formulation

Thus, all changes in the viewing parameters, are made according to an exponentially damped, sinusoidal slewing profile, in which the onset and offset of velocity are gradual, and the velocity is the largest midway. This profile is actually modeled after the time-response of a second-order, under damped system to a step input. Assume that a given viewing system parameter $x(t)$ is being modified. The actual path between the initial setting x_{old} and the final setting x_{new} is linear, and is given by:

$$x(t) = x_{old} + c(t)(x_{new} - x_{old}) \tag{4}$$

where $c(t)$ is a slewing function, varying between 0 and 1 and given by the following function of the time t:

$$c(t) = \frac{f(t)}{f_{\max}} \tag{5}$$

and $f(t)$ is the time response of a second-order system, with a unity DC gain, following a unity step input, according to:

$$f(t) = 1 - \frac{e^{-\pi \frac{t}{T_{slew}} \tan\phi}}{\sqrt{1-\zeta^2}} \cos\left(\pi \frac{t}{T_{slew}} - \phi\right) \tag{6}$$

and $f_{\max}$ is the peak value of $f(t)$, occurring at $t = T_{slew}$, given by:

$$f_{\max} = \left(1 + e^{-\pi \tan\phi}\right) \tag{7}$$

The angle ϕ is a phase shift angle due to damping and is defined as:

$$\phi = \tan^{-1}\left(\frac{\varsigma}{\sqrt{1-\varsigma^2}}\right) \tag{8}$$

where the parameter ς is the damping factor, $0 < \varsigma < 1$. The parameter T_{slew} is the 'slewing time', which is defined as the total time needed to complete the transition. It is also half of the period of the damped natural frequency ω_d:

$$T_{slew} = 0.5\omega_d; \quad \omega_d = \omega_0\sqrt{1-\varsigma^2} \tag{9}$$

where ω_0 is the undamped natural frequency. Note that $c(0) = 0$ and $c(T_{slew}) = 1$. Following Eq.(4) this means that at the start of the slewing action $x(0) = x_{old}$ and at the end $x(T_{slew}) = x_{new}$.

The slew-rate $\dot{f}(t)$ is obtained by differentiating Eq. (6):

$$\dot{f}(t) = \frac{\pi}{T_{slew}} e^{-\pi \frac{t}{T_{slew}} \tan\phi} \sin\left(\pi \frac{t}{T_{slew}}\right) \tag{10}$$

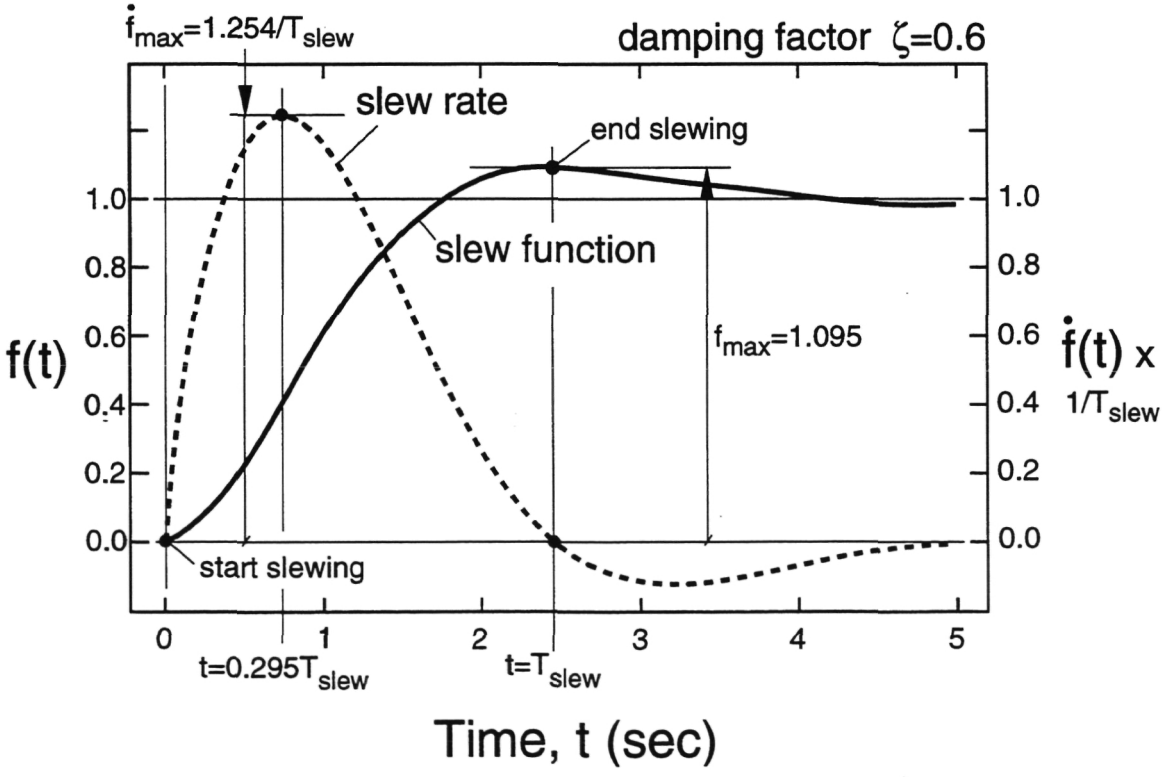

Figure 3.: Time histories of slew function and slew rate for $\zeta = 0.6$

The exponential term in Eq. (10) shows that the parameter ς causes an asymmetrical slew-rate profile, where the motion becomes the slowest towards the end. The damping factor ς determines how slowly the system slews-in on the terminal position. For $\varsigma = 0$ $\tan\phi$ is zero and the exponential term will be equal to one, so that the slew-rate profile will be symmetrical.

3.3. Time Histories of Slewing Functions

The time-histories of $f(t)$ and $\dot{f}(t)$ are shown in Fig. 3, for a damping factor of $\varsigma = 0.6$. The figure shows that the velocity is the largest mid-way, skewed towards the start of the operation, and decreasing towards the end. $f(t)$ reaches the peak value $f_{\max}$ at $t = T_{slew}$, which is the time at which $\dot{f}(t)$ is zero. It can be shown, by differentiating Eq.(10), that $\dot{f}(t)$ reaches a maximum at:

$$t_{\dot{f}_{\max}} = 0.5T_{slew}\left(1 - \frac{2\phi}{\pi}\right) \tag{11}$$

where the maximum $\dot{f}(t)$ is given by:

$$\dot{f}_{\max} = \frac{\pi}{T_{slew}} e^{-\left(\frac{\pi}{2}-\phi\right)\tan\phi} \cos\phi \tag{12}$$

It is clear from Eqs. (11) and (12) that for $\varsigma = 0$ $t_{\dot{f}_{\max}} = 0.5T_{slew}$ and $\dot{f}_{\max} = \pi / T_{slew}$. The time histories in Fig. 3 resemble the response of a well-designed servo-system, in which the slewed objects would have an actual mass or moment of inertia, and a proportional feedback law with position and rate feedback would reposition the object. The choice of this function greatly enhances the operator's impression that he, or she, is dealing with an actually existing physical system, rather than an abstract computer-generated scene which lacks the characteristics of the physical inertial world we are living in.

It should be noted however, that the implementation of the slewing function differs slightly from an actual servo system response. Following the overshoot and subsequent undershoot, the servo system output would settle on the final value of 1. The slewing function, however, is terminated at the peak-time, which is in this case at $t = T_{slew}$. Since the inclusion of the actual settling time response, following the peak value, would make the slewing process unnecessary longer, the slewing function was chosen to be terminated at $t = T_{slew}$.

Since computers are able to introduce viewing parameter changes in virtually zero time (e.g. the time needed for one background computation), slewing motions might appear to a system designer as unnecessary delay-introducing processes. However, discontinuities in the time-histories of viewing parameters are found to adversely affect spatial awareness and, in some cases, cause disorientation. The continuous slewing motion, however, allows the operator to actively 'follow' the viewing parameter change, from its initial setting to its final new situation. The association with a physically existing system which has distinct physical properties like mass or inertia, gives the operator the impression that the viewing parameter changes take place in a real physical environment, rather than an abstract computer-generated scene. By virtue of these slewing motions,

human characteristics, which are inherently present in the natural environment, can thus be utilized in the computer environment as well.

3.4. Determination of Slewing Parameter Values

A trade-off exists between the duration of the slewing process and the need for introducing natural viewing parameter changes. Too large slewing times might irritate the operator by introducing unnecessary delays in the process of setting viewing parameters. Too small slewing times might appear 'unnatural' and introduce disorientation. The choice of the slewing time would be the shortest time which still allows the operator to 'follow' the change along the way. Since larger changes demand larger slewing times, the slewing characteristics should be determined in terms of average slewing rates. These slewing rates however, should be expressed in screen coordinates, rather than real-world coordinates, since the actual stimuli associated with the slewing motions are perceived from the screen. Therefore the average slewing rates are defined either in degrees-per-second visual angle or pixels-per-second, measured on the screen.

3.4.1. Determination of the slewing time:

Prior to each viewing parameter change, the appropriate slewing time should be computed. For all viewing parameter operations the following process applies. The screen coordinates of a reference marker (in this case a manipulation pointer, discussed in detail hereafter), are computed for the 'old' and the 'new' viewing parameter setting. The distance between these coordinates, in pixels on the screen or degrees visual angle, is computed. The slewing time T_{slew} is chosen to be this distance, divided by the average slewing rate (in pixels-per-second or degrees-per-second, accordingly). The choice of the average slewing rate is highly empirical. Slewing rates in the range between 150-400 pixels-per-second are found to be adequate for all viewing system operations on a 20" diagonal monitor screen, measuring 1247 by 1024 pixels. However, this parameter should be fine-tuned for each operation individually through an experimental evaluation program.

Since small displacements take less time, a very small displacement is performed in almost zero time. This gives an erroneous impression of a 'jump'. Therefore, for the very small displacements, a minimum slewing time is defined. A value of 0.6 sec for the minimum slewing time is empirically chosen to be adequate for all viewing system operations.

3.4.2. Determination of the damping coefficient:

The choice of the damping coefficient ς is empirical as well. As mentioned earlier, ς introduces an asymmetrical velocity profile, where the system slows down towards the final position. The characteristic of the 'slowing down' towards the final setting is desirable, since it allows the operator to 'adjust himself to the new situation'. It also adds realism, by behaving like real physical servo systems, for which the slower motions towards the end are needed to achieve the necessary accuracy in the final positioning. On the other hand, too large values of ς will yield a too sluggish system. Adequate values are found in the range between $\varsigma = 0.6 - 0.8$. A slight adjustment of this parameter for each operation individually, might be necessary.

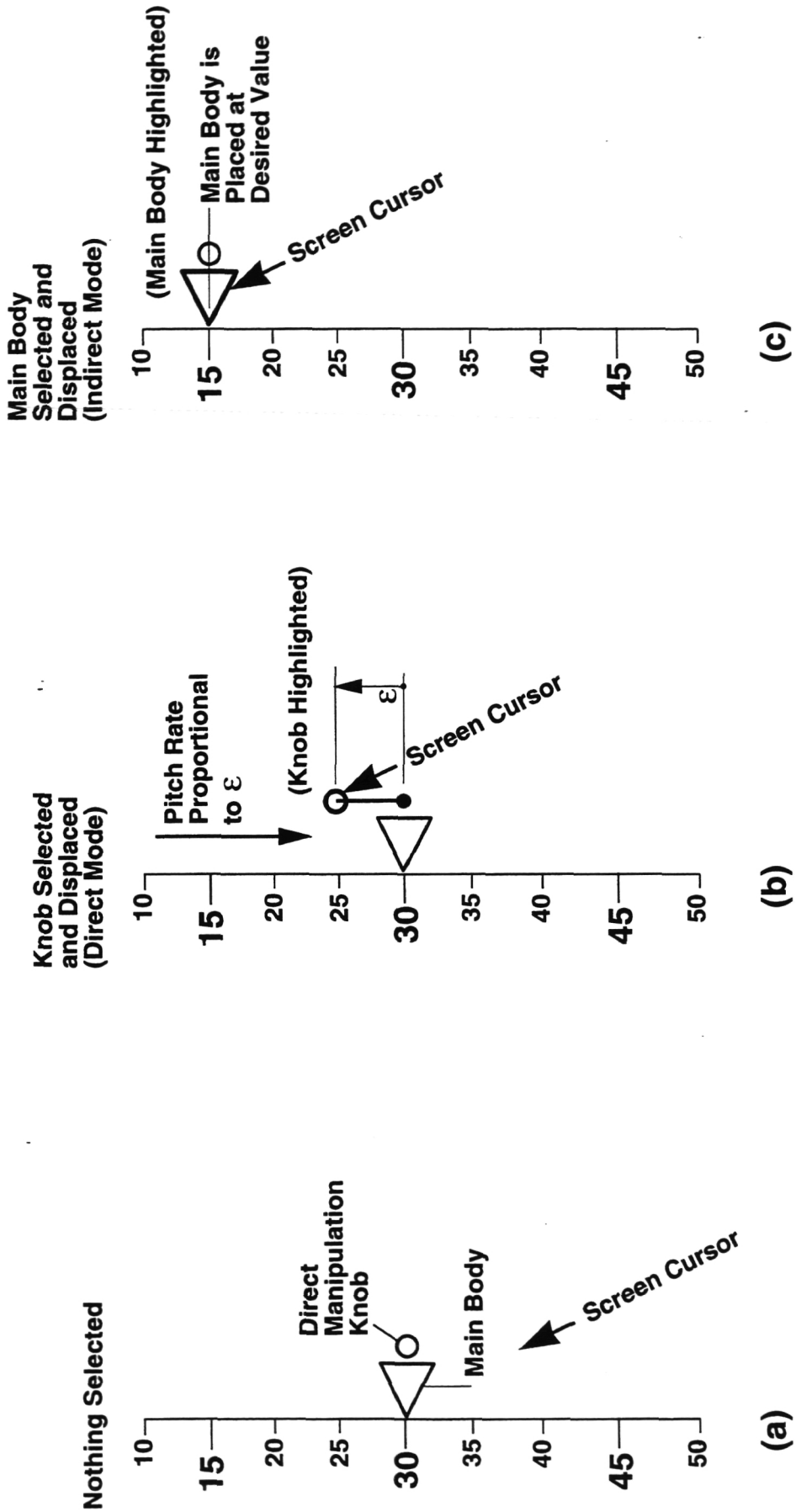

Figure 4.: Direct and indirect modes for manipulation pointers

3.5. Manipulation Pointers

Requests for changes in the viewing parameter settings are introduced by pointers (also called 'handles'). These pointers are an integral part of the 3-D scene, i.e. they have a defined spatial position. The manipulation pointers allow viewing parameter operations both in the *direct* and in the *indirect* mode, see Section 2.4. The method by which this is achieved is shown in principle in Fig. 4, for the vertical pitch adjustment. The manipulation pointer consists of two parts: the main pointer body, indicated by the left-pointing triangle, and the direct manipulation knob, as seen in Fig. 4a. Either the main body, or the knob can be selected.

Direct manipulation takes place by selecting the knob and displacing it in vertical direction. Since the main body will keep its position on the display, the knob will separate from the main body, as seen in Fig. 4b. The displacement ε between main body and knob constitutes the command signal for the change. Since pitch-angle changes are chosen to be rate-controlled, the pitch-rate in this case, is proportional to the displacement ε. In this example the system will reduce the pitch angle and the pitch scale will move downwards, in the direction of the arrow, see Fig. 4b.

Indirect manipulation takes place by selecting the main body and by dragging it to a location, opposite the requested pitch angle indicated on the pitch scale, as seen in Fig. 4c. The knob remains attached to the body. Note that the motions of pointers are restricted to their allowed workspace, since the main body as well as the knob can only move along a vertical axis. In addition, pointer motions are limited in magnitude in the sense that they can not be placed beyond the limits of the screen. This assures that the 'correspondence' between the new and the old setting will always be preserved. For example, a reversal of the viewing direction, which might lead to disorientation, will not be possible in one iteration.

3.6. Sequence of Operations

Pop-up menus are used to enter the manual viewing parameter setting mode. The menus generally appear, when clicking the mouse button, while nothing is selected. After entering the viewing mode, the manipulation pointers of all three viewing operations as mentioned in Section 2.3, will appear in the field. These pointers are discussed in detail hereafter.

Indirect manual viewing parameter operations are performed in three steps: (1) choosing the operation, i.e. translate, rotate or ranging by selecting the appropriate pointer; (2) positioning the pointer at the required 3-D position; (3) executing the actual change by means of a controlled slewing motion. During this operation the pointer returns to its initial home position.

3.6.1. Choosing the operation by selecting the appropriate pointer:

Selection of the pointer takes place by 'touching' the pointer with the screen cursor. It is not necessary to press the mouse button for selecting these pointers. Identical to the selection of all other objects on the display, the selected pointer will be highlighted (a change in color and an increase in line width will take place). By moving the screen cursor away from the pointer, the pointer will again become 'de-selected' and no changes will have taken place. As soon as a pointer has been selected, the operator has activated the particular operation, i.e. translate, rotate, or ranging. The pointers and symbology of the other non-active operations will disappear, and the scale of the selected operation will be expanded.

3.6.2. Positioning the pointer:

If a pointer has been selected (appears with a bright color), and the mouse button has been pressed and held down, the pointer will become *attached* to the cursor. This means that the pointer will follow the cursor, to the extent that the pointer motions remain within their allowed degrees-of-freedom. Thus, for example, the 'focus-of-interest' pointer can not leave the ground plane, the yaw-rotation pointer can only slide horizontally along the yaw-scale, etc. The screen cursor itself, on the other hand, will never be constrained in its motions and can be placed at any 2-D location, within the screen boundaries.

3.6.3. Enhancement of the screen cursor:

In order to ensure that the operator remains aware of the fact that he, or she, is actually manipulating the screen cursor, rather than, for example, the position pointer in the ground plane, it is essential to enhance the screen cursor during drag operations. This enhancement is achieved by enlargement of the screen cursor. The need for this enhancement is demonstrated as follows. When the pointer and the cursor become attached to each other, it becomes less clear to the operator which one of the two is being manipulated. In case both the pointer and the cursor operate in the same 2-D workspace, e.g. for a position pointer, moving in the ground plane viewed straight from above, it doesn't really matter which one of the two is being manipulated by the operator, since the *xy*-motions of the mouse have an identical effect on each one of them.

However, in a perspective display, the workspace of a position pointer in the ground plane will be basically different from the workspace of the mouse. This is demonstrated as follows. Since the position pointer is constrained to the ground plane, it will not be possible to position it above the true horizon (for flat earth). The screen cursor, though, is not constrained and can be placed anywhere above the horizon. The solution to this problem is to constrain the workspace of the position pointer such that it remains within a given maximum 'no-follow' range, ahead of the actual 'focus-of-interest'. In practice this means that the position pointer simply stops following the screen cursor, when it is requested to leave its workspace.

3.6.4. Executing the requested change:

Execution of the change in the indirect mode takes place by releasing the mouse button. A 'slewing motion' is initiated during which the relevant viewing parameters are transitioned to the new requested values. In practice this means that the pointer will remain 'fixed' in the 3-D scene and slew back to its home position, following the changes taking place in the viewing parameters. The pointer thus constitutes a 'key reference point' during the transition to the new viewing parameter setting. The operator is able to see and follow the pointer along its path during the transition, which will contribute to his or her understanding of the operation and minimize the risk for disorientation. Since during the transition period the pointer constitutes the essential reference and since the operator has no control over the pointer, the less relevant screen cursor is blanked. After the slewing motion has been completed, the screen cursor will re-appear at the same position relative to the pointer, identical to the one before the start of the transition operation.

4

DESCRIPTION OF DISPLAY

4.1. Selection of Objects

All objects in the field (aircraft symbols, Air Traffic Control symbology, pointers, etc.) are subject to selection by the screen cursor. The motions of the screen cursor are unconstrained and have a fixed gearing with the 2-D control device (mouse). Objects are selected by touching them with the screen cursor. In all cases the system acknowledges that the object is selected, e.g. by changing its color, intensity, line width, etc. There is no need for pressing the mouse button in selecting objects. Apart from the acknowledgment of selection, no actions are taken by the system, provided the mouse button is not pressed. The object is de-selected by simply moving the mouse cursor away from the object.

Objects are arranged by object type, item and group. For example, all aircraft symbols belong to the group 'vehicle icons' and might be of various types, like 'heavy transport', 'light aircraft' or 'rotary wing', etc. A number of aircraft of the same type might be present in the area. Each individual aircraft is identified by an 'item' number.

Four levels of selection exist. The first level, full-body selection, takes place when the screen cursor touches any part of the object's body. The second level, selection by selection circle, takes place only when the screen cursor touches a circle, centered at the object. In the third level, the selection is disabled, although the object will be visible. In the fourth level, non-visible objects can be selected. This level is useful for testing whether the screen cursor is located within a certain area of the groundplane or in a certain area of the display. In addition, priority levels can be set. If the cursor simultaneously touches a number of objects, only the object with the highest level of priority is selected.

4.2. Menus and Menu Operations

The system modes are controlled through pop-up menus. Pop-up menus for controlling the system modes appear, when the mouse button is pressed, while no objects are selected. Task-specific pop-up menus will be used when the mouse button is pressed while a specific object is selected.

The main menu appears in the main program mode, when the mouse button is pressed while no items are selected. Selection takes place by moving the screen cursor to the desired option and by releasing the mouse button. If the mouse button is released, while no selection has been made, the menu will remain visible. The menu of the main mode allows branching to other program modes and also includes the path for exiting the system.

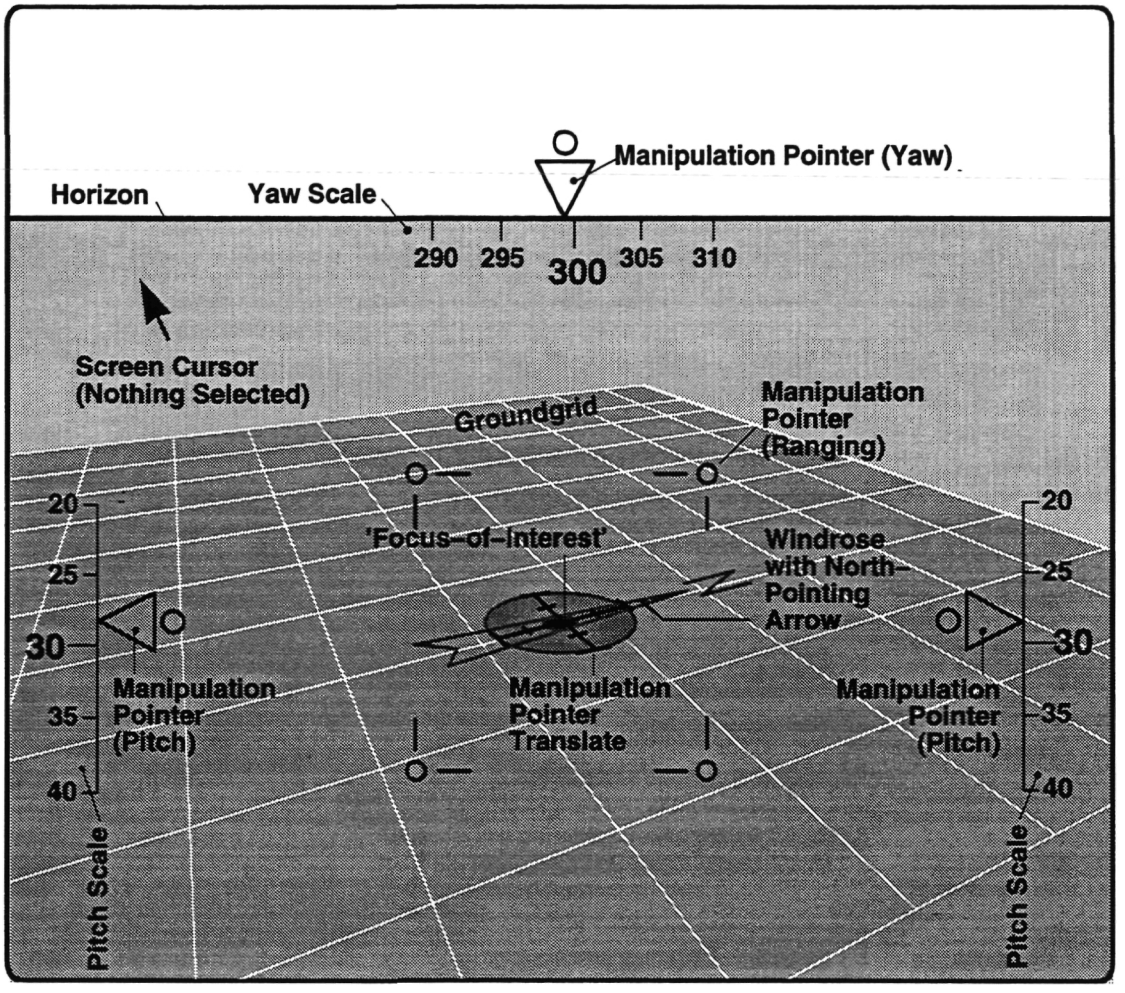

Figure 5.: General screen image in the viewing mode

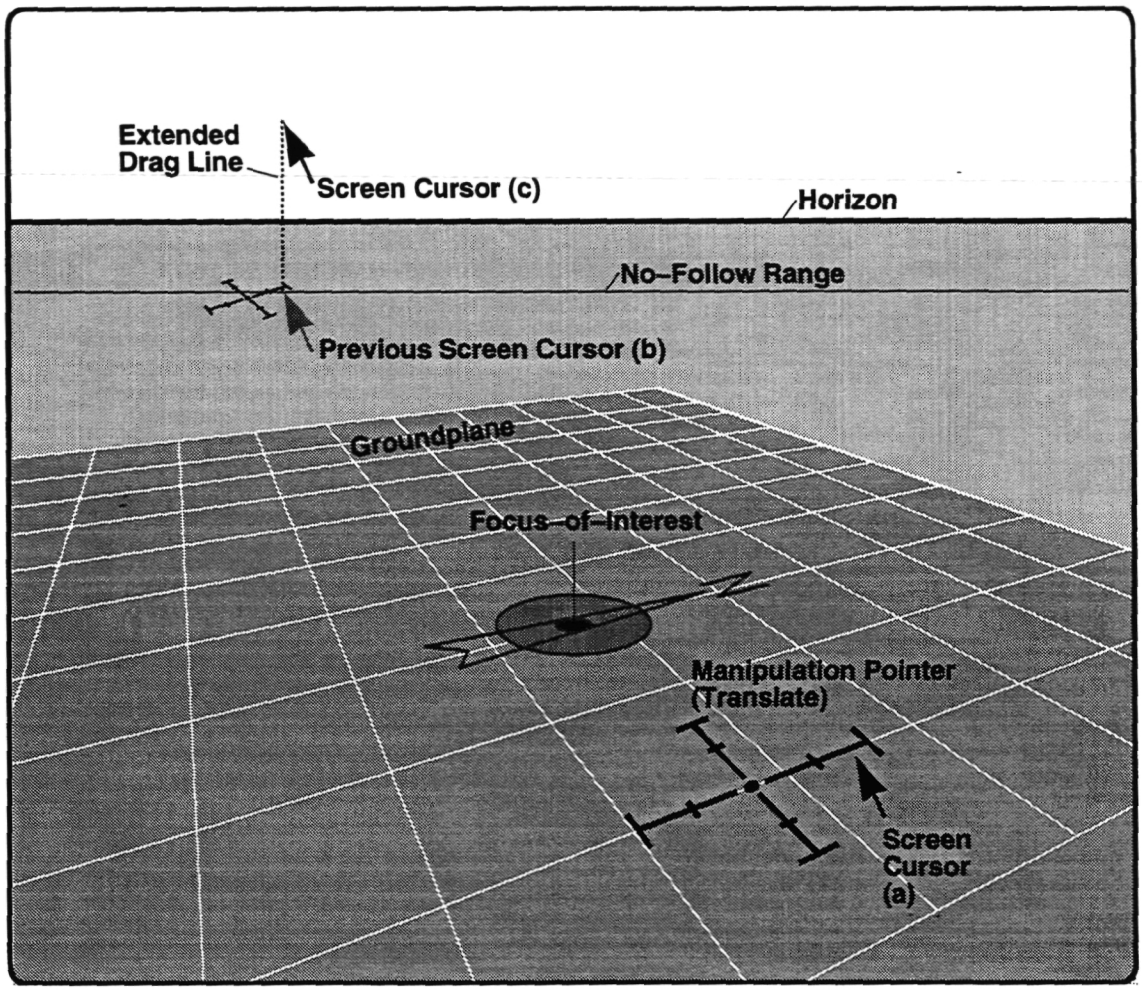

Figure 6a.: Manipulation pointers for *indirect* translate operations

4.3. Manual Viewing Parameter Setting (MVPS) Operations

Each one of the three MVPS operations, i.e. translate, rotate and range, has specific manipulation pointers and reference scales associated with them. The general sequence of operations of selecting and positioning the pointers, and of executing the viewing parameter change, has been outlined in Section 3.6. Manipulation pointers are selected at a 'full-body' level, i.e. the selection takes place when the screen cursor touches any part of the pointer. In the repositioning phase, the pointer will remain attached to the screen cursor at the same 3-D relative position at which it was first touched by the screen cursor. The manipulation pointers for each one of the MVPS operations, are described in detail hereafter.

The general screen image in the viewing mode is shown in Fig. 5. This image is presented when no items are selected, i.e. no specific viewing operation has yet been chosen. In this mode the manipulation pointers of all three operations are visible, as well as shortened scales for the azimuth and elevation adjustment. The scale at the top of the display is the azimuth (yaw) scale, which normally coincides with the horizon, in case the horizon is visible. An angle of 360 degrees depicts the magnetic north. In the presence of elevation angle adjustments, the horizon will move vertically, and the azimuth scale will remain attached to it. In case the elevation angle is so large that the horizon is no longer within the field-of-view, the azimuth scale will detach itself from the horizon, and remain at a fixed vertical position at the top-edge of the display.

The two vertical scales at the sides are the elevation (pitch) scales. An elevation angle of 90 degrees depicts that the groundplane is viewed vertically, i.e. a plan view. The four corner tic-marks in the central area of the display constitute the pointers for manipulating the ranging parameter. In the groundplane the center of the windrose with the north-pointing arrow symbolizes the 'focus-of-interest' about which the viewing axis is rotated.

4.3.1. Translate mode:

(a) Indirect operations:

The manipulation pointer for *indirect* operations in the translate mode is shown in Fig. 6a as a reference cross. Initially, this cross is located at the 'focus-of-interest' about which the viewing axis is rotated. As mentioned earlier, the 'focus-of-interest' is indicated by the windrose with north-pointing arrow. The cross is located in the ground plane and drawn locally-level at all times, and aligned with the north-south east-west grid directions.

In this case the ground plane is represented by a flat surface. However, for non-flat structured 3-D terrain, the manipulation pointer should follow the contours of the terrain.

The cross can be moved around the ground plane (or along the 3-D surface in case of non-flat terrain) by the screen cursor. It should be noted that although the motions of the screen cursor are slaved to the 2-D motions of the control device, the cross moves in 3-D space. Consequently, the cross will change, both in size and shape, as it is moved along the surface. The actual viewing parameter change will be executed by means of a slewing motion, during which the pointer will be returned to its home position.

Since the cross symbolizes the position of an object in 3-D space, the operator might erroneously map the *xy*-motions of the control device into 2-D motions along the grid lines of the ground plane. This potentially confusing situation is avoided by enhancing the screen cursor during the relocation of the cross in the ground plane. The enhanced presence of the screen cursor will remind the operator that it actually is the screen cursor which is manipulated by the 2-D control device, rather than the cross itself.

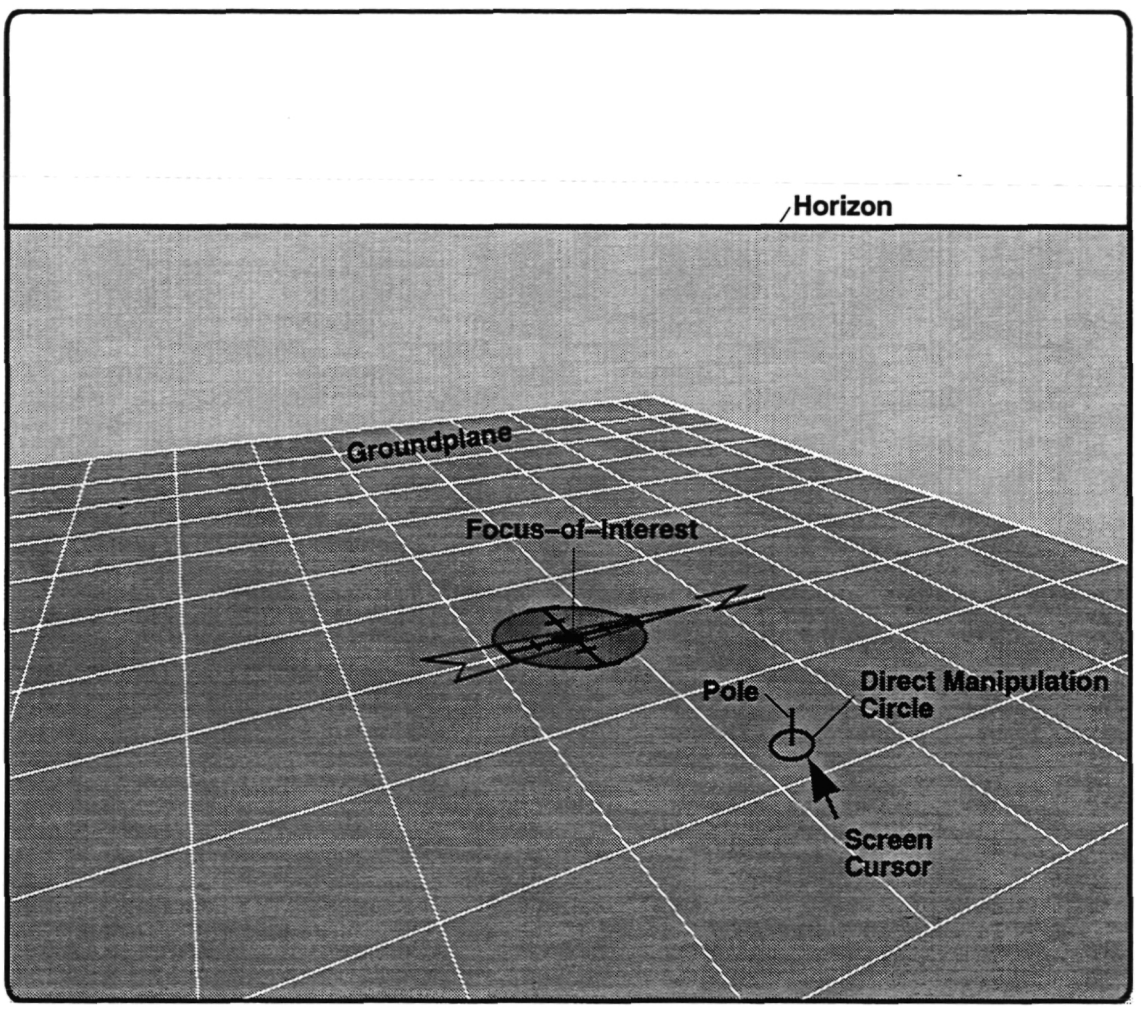

Figure 6b.: Manipulation pointers for *direct* translate operations

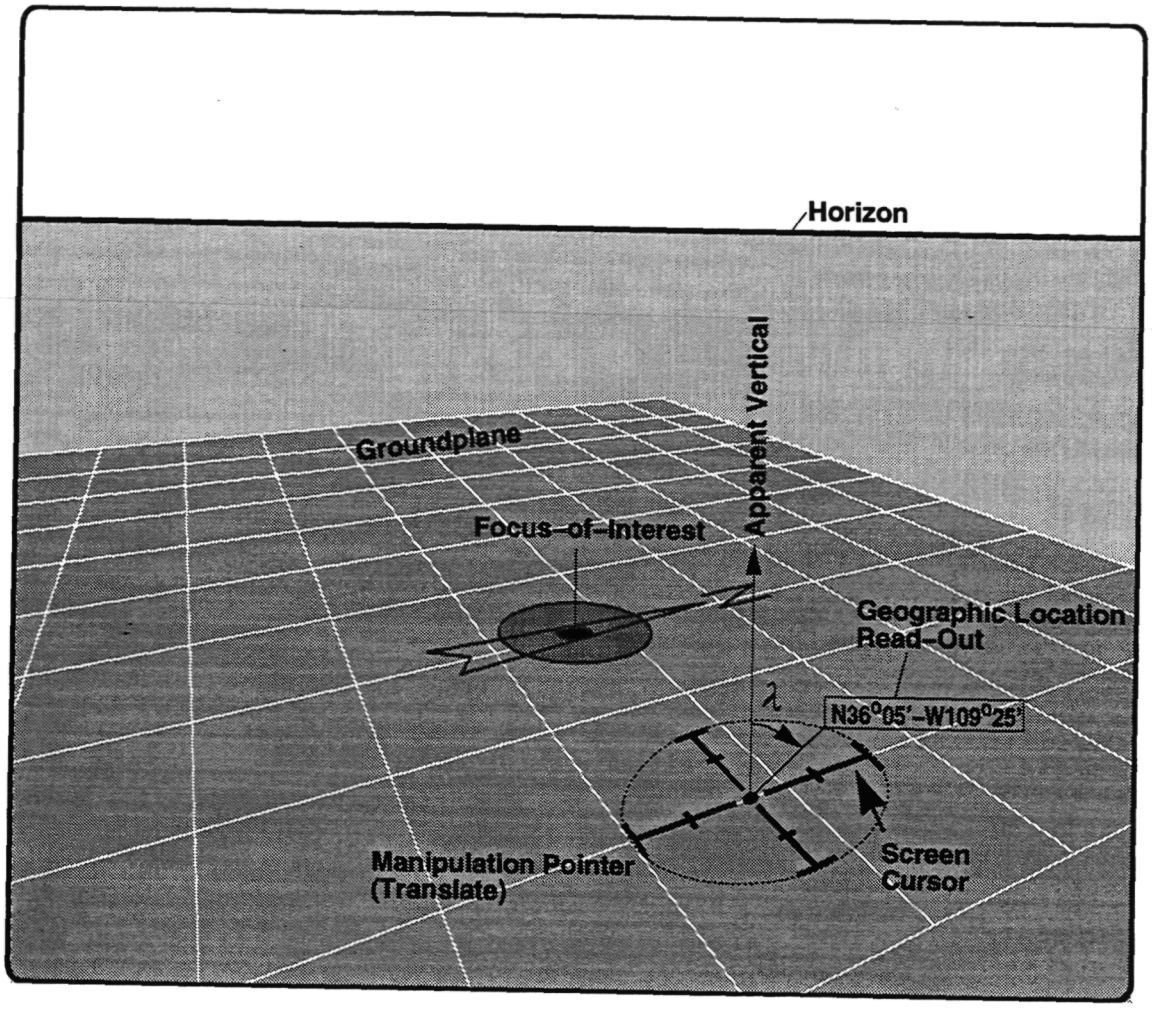

Figure 7.: Digital position read-out in the translate mode

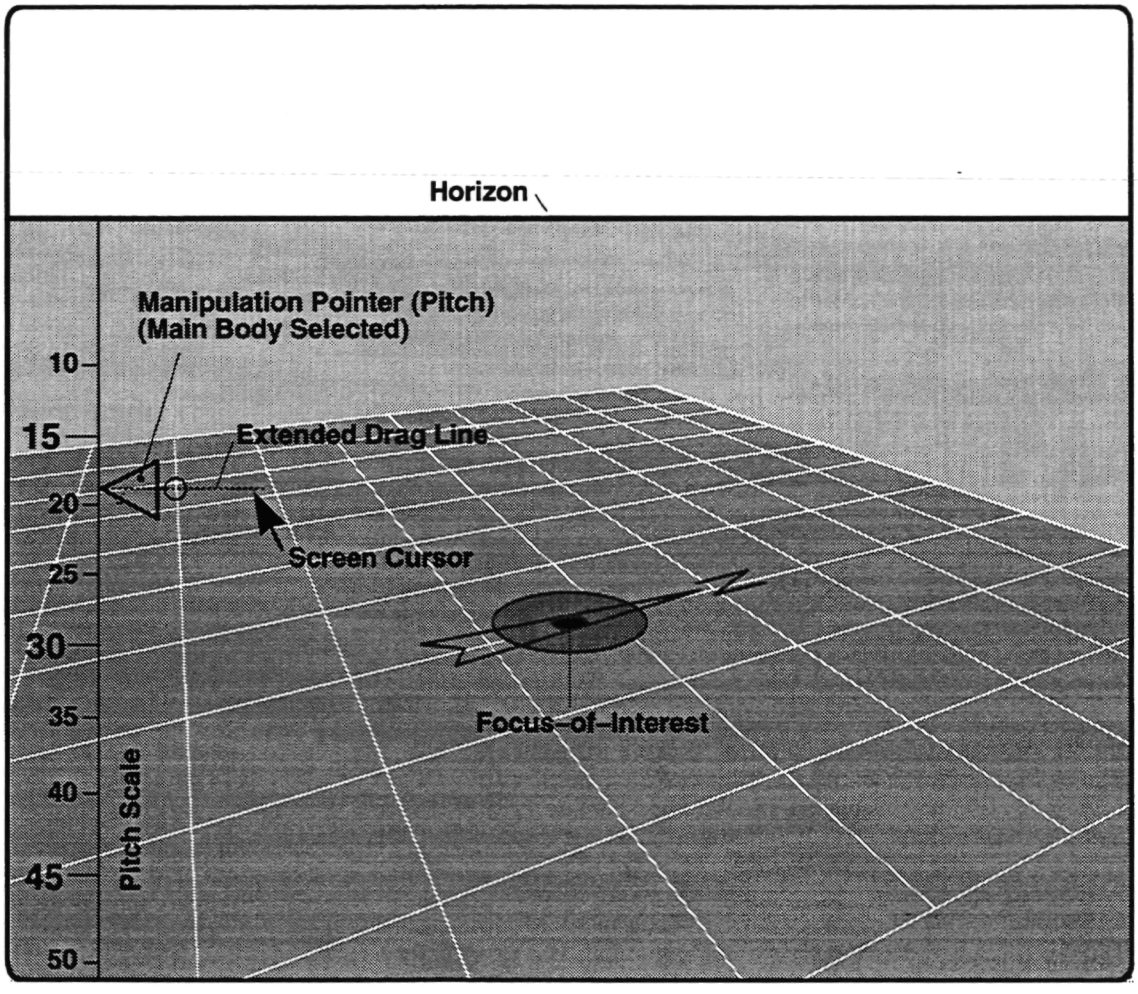

Figure 8a.: Manipulation pointers for the rotate mode; *pitch* operations

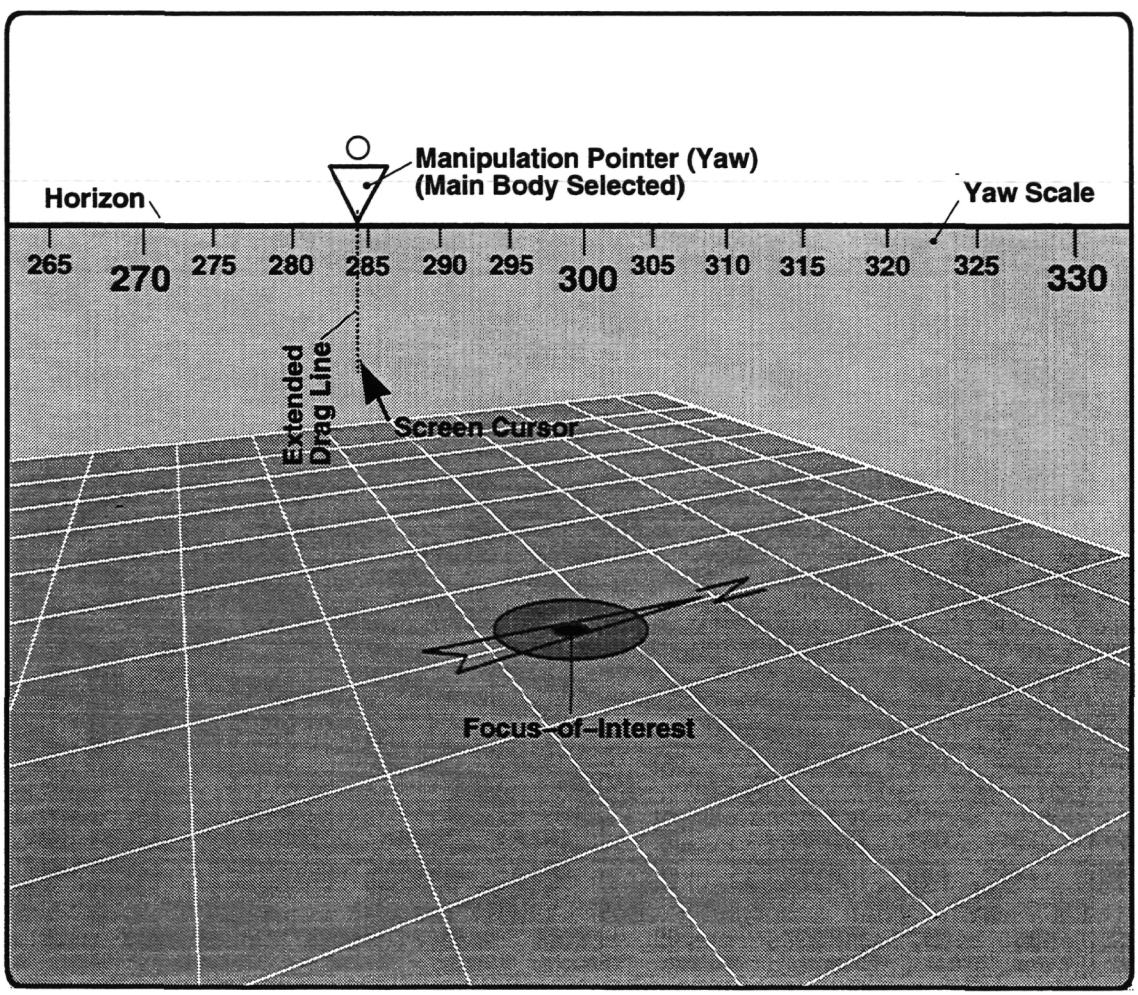

Figure 8b.: Manipulation pointers for the rotate mode; *yaw* operations

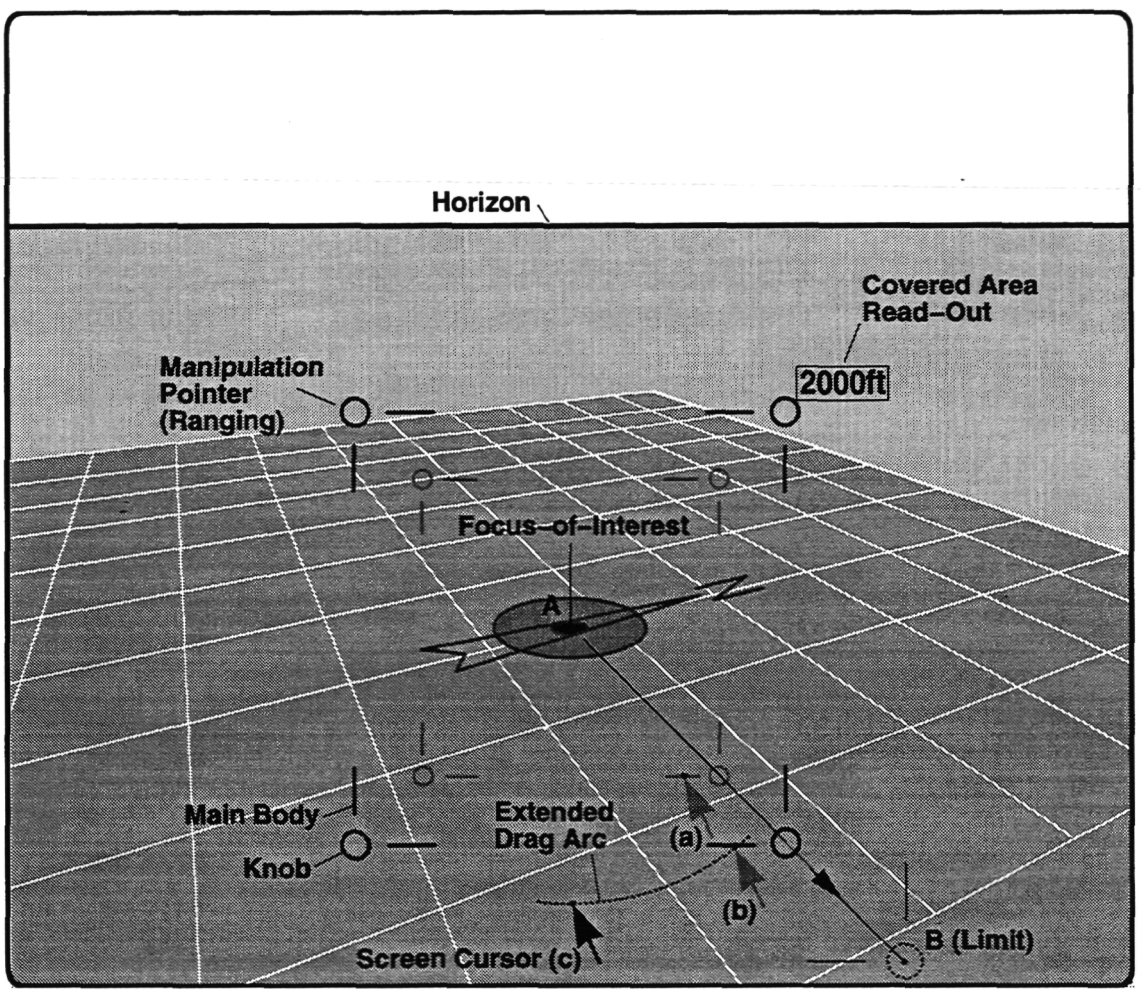

Figure 9a.: Manipulation pointers for *indirect* ranging operations

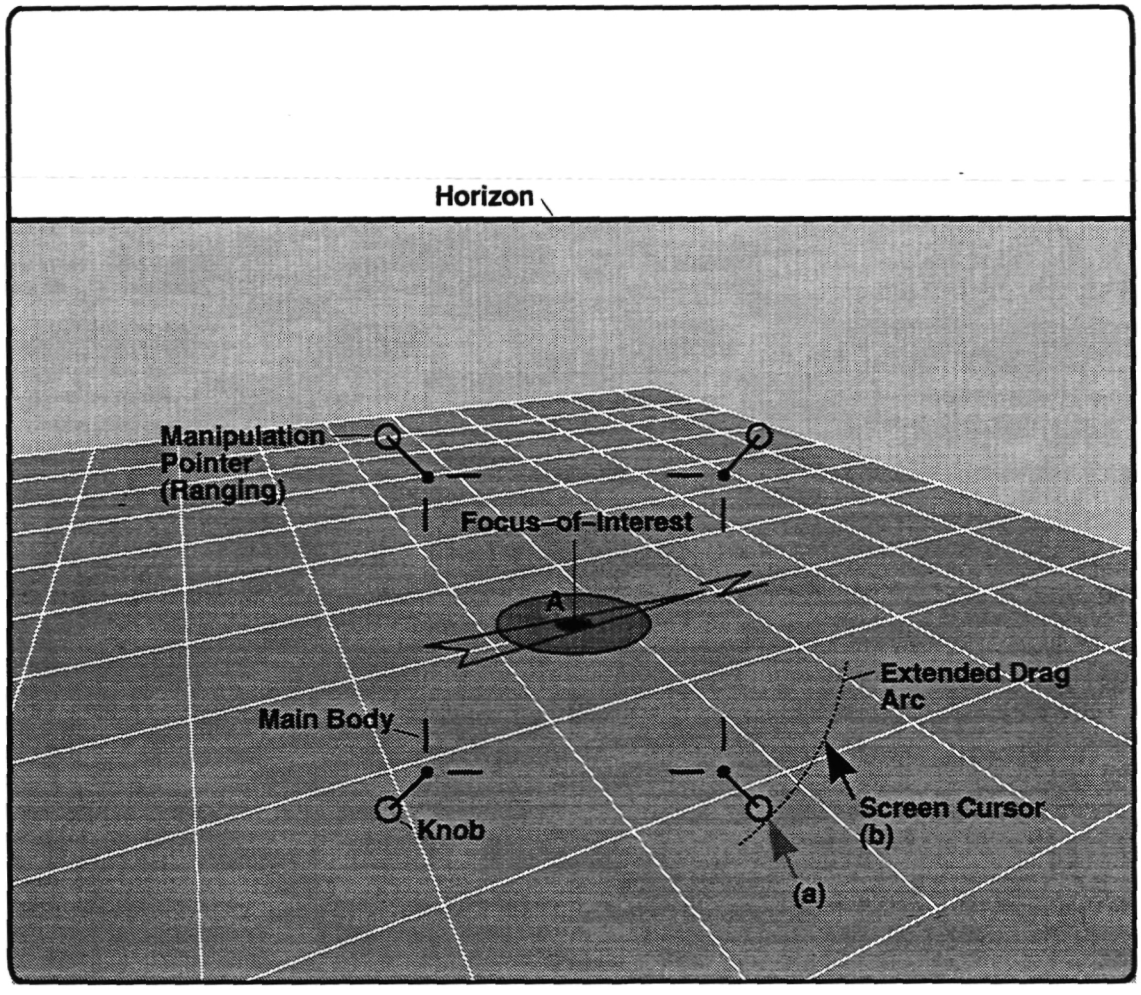

Figure 9b.: Manipulation pointers for *direct* ranging operations; ranging out

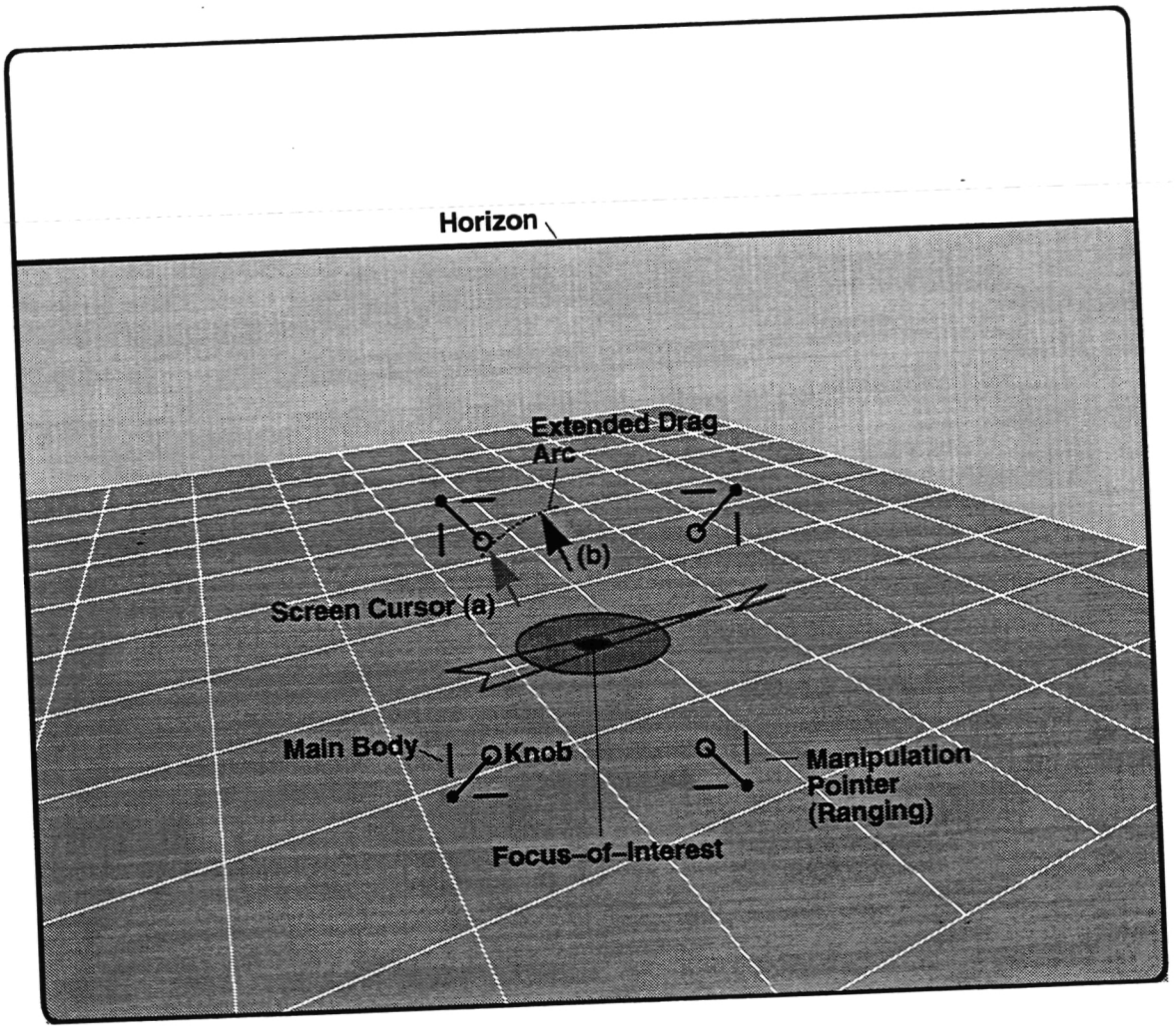

Figure 9c.: Manipulation pointers for *direct* ranging operations; ranging in

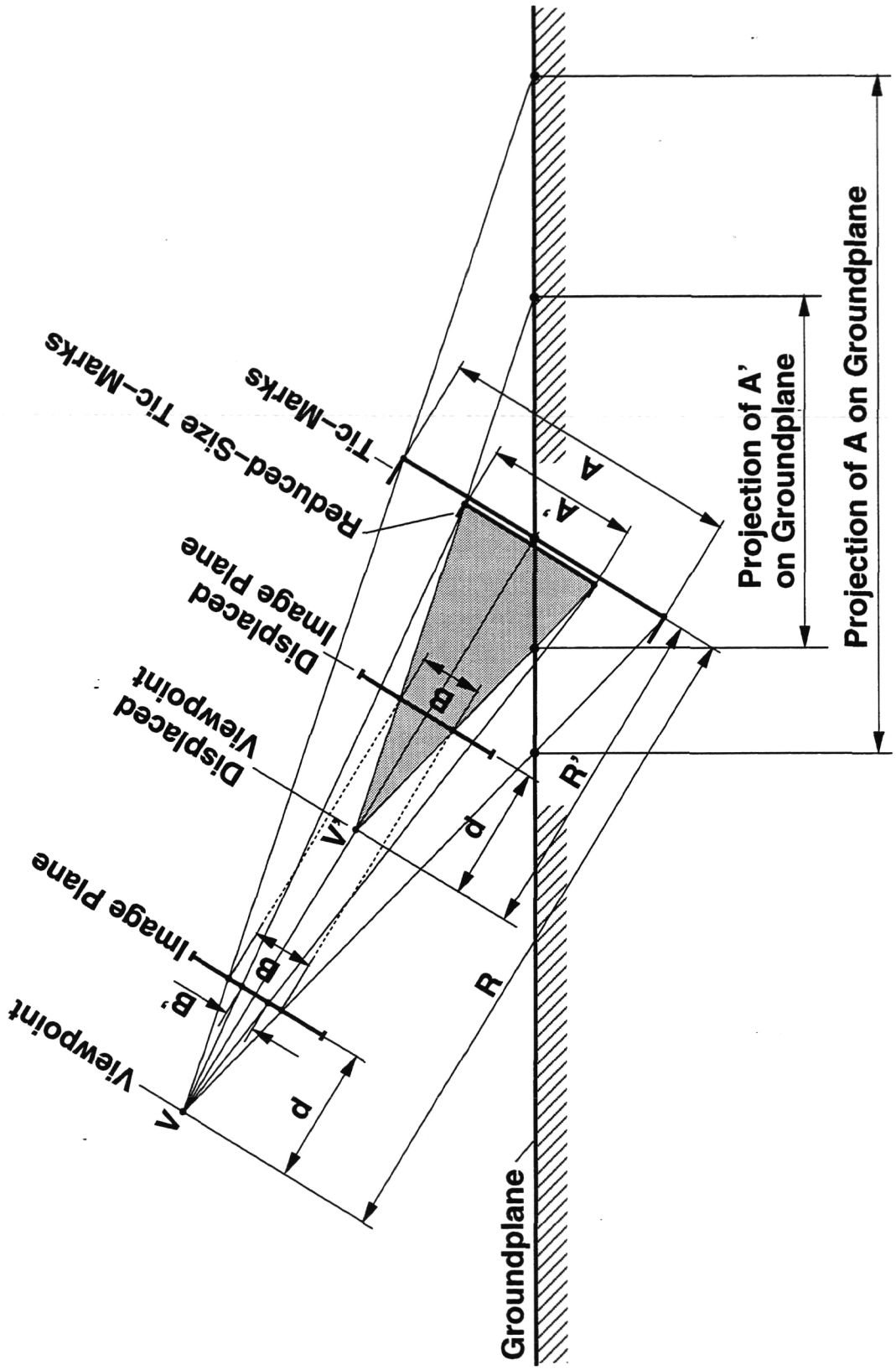

Figure 10.: Geometry of ranging operation

As outlined in Section 3.6.3., the position pointer can not leave its allowed workspace. Thus, the pointer will not follow the screen cursor, if it would be required to cross the 'no-follow' range. This is demonstrated in Fig. 6a. The screen cursor has moved from position (a) to position (b). At position (b) the position pointer has reached the 'no-follow' range. At position (c) the screen cursor has moved above the dotted 'no-follow' range line. An extended 'drag line' appears, subtended between the cursor and the previous point of attachment. The pointer will still follow the cursor in the lateral motion, but not in the vertical one.

(b) Direct operations:

Direct translate operations take place by direct manipulation of the groundgrid. When the screen cursor is located within the groundgrid, the direct manipulation circle will be visible at its endpoint, as shown in Fig. 6b. When the mouse button is not pressed, this circle can be moved freely over the groundplane. Since the circle is spatially located in the groundplane, it follows the same rules of perspective as the indirect manipulation pointer cross.

As soon as the mouse button is being pressed, a vertical pole will appear at the center of the circle, the circle will be highlighted and the screen cursor enhanced. The circle will now be 'locked' on the groundplane and the groundplane will be displaced in accordance to the motions of the circle. Note that this arrangement allows a natural way for making 'course' and 'fine' adjustments. When the circle is being locked on the groundplane at close range, following the rules of perspective, large screen cursor motions will induce small displacements of the groundplane. The opposite is the case, when the circle is locked on the groundplane at far-away range.

While moving the manipulation pointer on the screen, a digital read-out of the geographic location (in standard Earth latitude and longitude angular coordinates) of the pointer is displayed, as shown in Fig. 7. In order to avoid clustering of this information with the cross itself, the data string is positioned with its lower-left corner at the outer circle, enveloping the cross. The heading of this corner with respect to the center of the cross is obtained by adding the fixed angle λ to the viewing direction indicated by the apparent vertical line, in clockwise direction.

The actual size of the pointer in terms of units of length measured in the ground plane, is kept fixed during translate operations. However, this size is scaled according to the viewing range. Thus, if the ground plane were viewed straight from above, the size of the pointer in screen units, as it appears on the screen, would be unaffected by the viewing range. A similar scaling takes place for the slewing motions. Thus the slewing rate, in pixels per second, will be independent of the viewing range.

4.3.2. Rotate mode:

(a) Indirect operations:

Manipulation pointers for the rotate mode are shown in Fig. 8a and 8b, for the elevation (pitch) and azimuth (yaw) rotation, respectively. The motions of the pointers are limited to their allowed workspace. Thus, the pointers for setting the elevation angle can only move along the vertical pitch scales and the pointer for setting the viewing direction azimuth, can only move along the horizon.

The pointer, moving along the vertical scale at the left side of the display, is used to set the viewing elevation angle, i.e. the angle Θ_{los}, as seen in Fig 8a. Note that either one of the pitch scales could have been used to set the viewing elevation angle. The screen-cursor does not necessarily have to remain in close contact with the pointer. In the example in Fig. 8a the screen cursor has been moved to the right and the pointer will still follow the cursor in the vertical direction by means of the extended drag line. When the pointer is at rest, the adjacent numerical indicates the viewing elevation angle. For example, an angle of 90 degrees indicates that the ground plane is viewed perpendicularly.

The pointer, moving along the horizontal yaw-scale located at the horizon, is used to set the azimuth angle of the viewing direction, i.e. the angle $\Psi_{los} + 180^{o}$, as seen in Fig. 8b. When the pointer is at rest, the numerical below the pointer indicates the viewing direction azimuth angle, measured clock-wise positive from the north. Also in this example the screen cursor has been moved in downwards direction, and the pointer will still follow the cursor in the horizontal direction by means of the extended drag line.

The viewing parameter change is initiated by selecting the appropriate pointer, and by dragging it to the desired viewing azimuth or elevation. The actual change will take place by an appropriate slewing motion, during which the pointer will be returned to its home position.

(b) Direct operations:

Direct translate operations take place by selecting and displacing the direct manipulation knob on the pointer. As outlined in Section 3.5 the displacement of this knob from the main body will result in a proportional angular rate in pitch (when the pitch pointer knob has been selected), or a proportional angular rate in yaw, (when the yaw pointer has been selected).

4.3.3. Range mode:

Manipulation pointers for the range mode are shown in Fig. 9 as the four tick-marks of a rectangle. Similar to the rotation pointers, the ranging pointer is composed of a main body and a direct manipulation knob. The knobs are at the vertices of the tic-mark rectangle.

(a) Indirect operations:

Indirect ranging operations take place by reducing or enlarging the area, closed-in by the tic-marks. The geometry of the ranging operation is shown in Fig. 10. The tic-marks are supposedly located in a plane perpendicular to the viewing vector, and centered at the focus-of-interest, as seen in Fig. 10. If the ground plane were viewed perpendicular, the tick-marks would enclose a rectangular area of given dimensions A. The size of the area enclosed by the tic-marks, as it appears on the image plane, is denoted by B.

In Fig. 10. The tic-mark area is reduced in size from size A to size A'. Consequently, size of the tic-mark area as it appears on the image plane, will be reduced as well, i.e. from B to B'. The change is executed by slewing the viewpoint V along the viewing axis, to its new location V'. Point V' is the location, at which the reduced tic-mark area A' will appear on the image plane at the same size B, as it had before the change. The ranging operation is thus also consistent with the other viewing parameter operations in the sense that at the completion of the execution of the change, the manipulation pointers have returned to their home position.

Selection takes place by touching any one of the four corner tic-marks with the screen cursor. Situation (a) in Fig. 9a, shows the screen cursor attached to the lower-right tic-mark. Since the tic-mark area can only be reduced or enlarged in size, i.e. it can not be reshaped, the workspace of the tic-mark of situation (a) is restricted to motions along the line, subtended between points A and B, (points A and B are the 'no-follow' limits). The motion of the other three tic-marks will be such, that the original shape of the tic-mark area will be maintained.

Situation (b) in Fig. 9a shows that the tic-mark area has been enlarged. In situation (c) the screen cursor has been moved away from the allowed tic-mark workspace to the left. Similar to the position and rotate pointers, an 'extended drag arc' appears (with its center at the focus-of-interest), which allows the pointer to follow the screen cursor, while remaining on the line AB, i.e. while staying within its allowed workspace.

While moving the manipulation pointer on the screen, a digital read-out of the width of the covered area is displayed, as shown in Fig. 9a. This value is in fact the width of the tic-mark area on the ground plane, if the ground plane were viewed perpendicular. The data string is centered with its lower-left corner at the upper-right tic-mark.

(b) Direct operations:

Figs. 9b and c show direct ranging operations. In Fig. 9b the lower-right knob is displaced in outwards direction. The other three knobs will be displaced as well, such that the original shape formed by the four knobs will be maintained. The system will range-out, i.e. enlarge the range, at a rate proportional to the displacement of the knob from the main body. In Fig. 9c the upper-left knob is displaced in inward direction. Consequently, the system will range-in, i.e. reduce the range at a rate proportional to the displacement of the knob from the main body.

4.3.4. Reset and return options:

As mentioned earlier, reset and return operations are initiated through the 'View Options' menu. This menu appears while in the MVPS mode, and no pointers are selected. The 'Return' option returns the system to the mode from which the MVPS mode was initiated, i.e. here the main program mode.

The 'Reset' option will allow the viewing parameters to be reset to a given initial setting, or preferred viewing situation.

5

AUTOMATED VIEWING PARAMETER SETTING

5.1. Automated Viewing Parameter Setting (AVPS)

Automated viewing parameter setting schemes employ an optimization strategy, aimed at identifying and realizing the best possible vantage point, from which the Air Traffic Control scene can be viewed, for a given traffic situation. The scheme is intended to contribute to overall system performance in the following manner:

1. It directs the operator's attention to critical areas in the field, by viewing these areas centrally and from a nearby distance, while at the same time maintaining a global view over large, less critical areas, by viewing these areas from far away in the periphery.

2. It prevents clutter, or exclusion from the view, of one aircraft symbol by another one, by modifying the viewing parameters such, that each one of the aircraft in the critical area appears separated from the other.

3. It finds a compromise between the accuracy, at which horizontal and vertical relative positions can be estimated, e.g., a plan view provides the best horizontal relative position information, but does not provide relative vertical position information, whereas the opposite is the case for a side view.

The scheme will include the following main components:

1. An algorithm, which employs an optimization strategy for finding the optimal viewing parameter setting for a given traffic situation.

2. A decision algorithm, which decides, based on the current situation, the current viewing parameter setting, the computed desired optimal setting, and the time-span elapsed since the last change, whether a change in viewing parameter setting should indeed be initiated.

3. A path-planning algorithm, which determines the spatial path as a function of time, along which the change in viewing parameters should be made. Since viewing parameter operations might involve changes in a number of variables, the spatial path might be complex. The path should be planned such that the change will not negatively effect the spatial awareness of the operator. This algorithm will employ the 'slewing functions' in order to ensure gradual transitions.

5.2. Design Requirements for AVPS Operations

Basic design requirements for AVPS operations are:

1. AVPS activities are initiated only when absolutely necessary. This will require the definition of threshold values, below which AVPS activities are not initiated. These values will be incorporated in the decision algorithm.

2. AVPS activities are executed intermittently. This will require the definition of a minimal allowed time-span between operations. The intermittent operation will give the operator the impression of viewing the scene mostly from a stationary viewpoint, with occasional, short-lasting changes. This will allow the operator to differentiate between motions of objects in the field, and motions due to the viewing parameter changes. The minimal allowed time-span between operations will also be incorporated in the decision algorithm.

3. AVPS activities are subject to limitations in magnitude of viewing parameter changes. Typically, changes, exceeding the ones which would occur in manual *indirect* viewing parameter setting (MVPS) operations, should be avoided. However, the choice of an appropriate spatial path might allow changes which are larger than sequential (one parameter change at the time) MVPS operations.

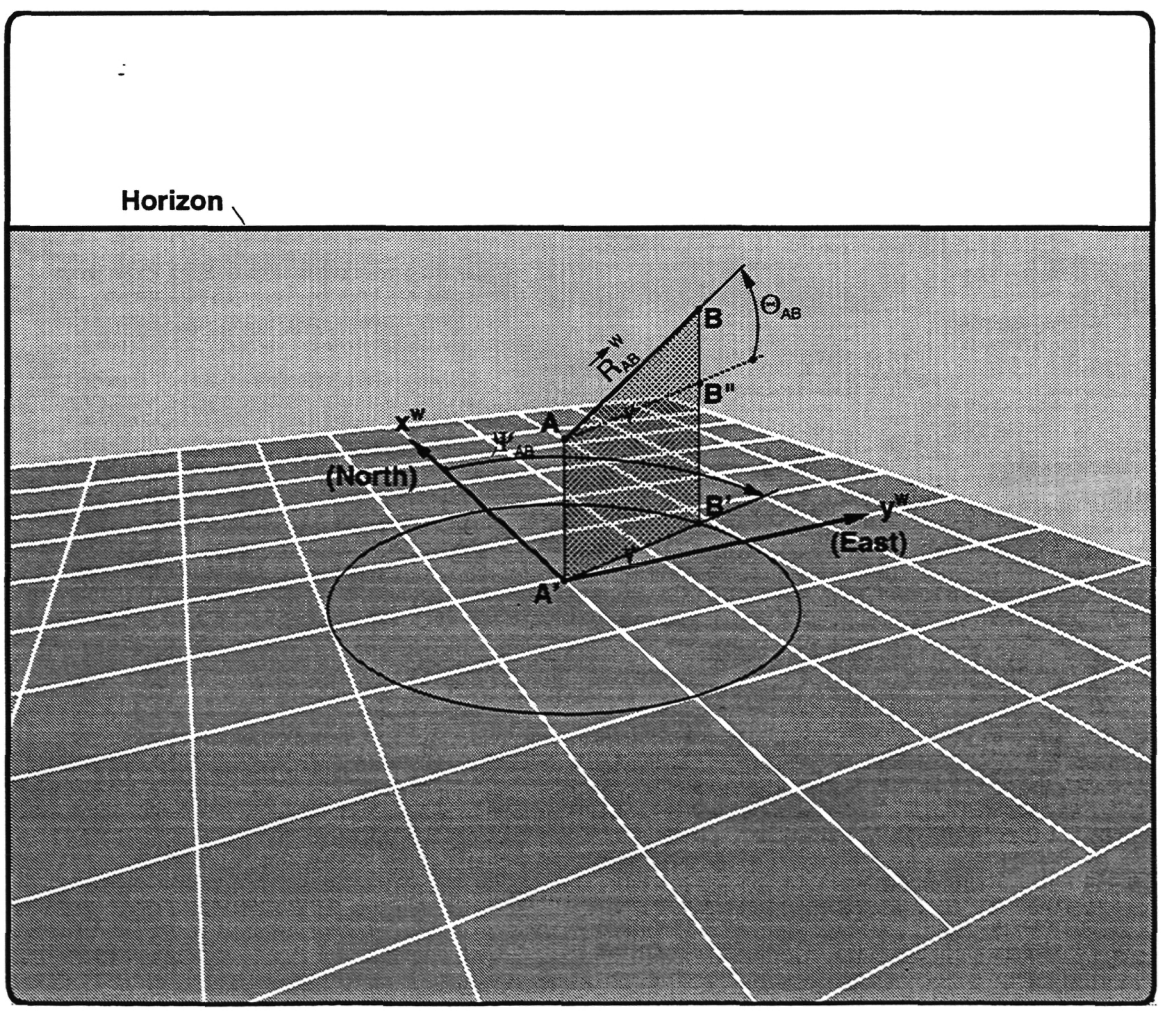

Figure 11.: Perspective view of two spatially separated aircraft

5. The operator must have the authority to override the AVPS activity manually at all times, i.e. stop a certain activity in the middle, return to a previous setting, etc. AVPS activities will be imparted to the manipulation pointers. The operator will experience the AVPS changes as if 'a skilled assistant operator' would manipulate the pointers.

6. MVPS operations will be possible also when the AVPS system is engaged. Thus, MVPS activities will take priority over AVPS operations. AVPS activities will resume a minimal allowed time-span after the MVPS activity has been completed and use the new setting as the baseline for their computations. Knowledge of the existence of MVPS activity will be imparted to the decision algorithm as well.

5.3. Principle of Operation of the AVPS

The algorithm, which employs an optimization strategy for finding the optimal viewing parameter setting for a given traffic situation, is based on the minimization of a global cost function J. This global cost is composed of two parts: J^1 and J^2. The first part, J^1, relates to the location on the image plane, at which the aircraft symbols appear. For example, a large cost should be attributed to aircraft which should be given a high level of attention and which should appear in the center of the display, but which are actually displayed far-off to the side. Minimizing the first part of the cost would mean choosing viewing parameters which would tend to move these aircraft to the center of the display.

The second part, J^2, comprises the sum of all individual costs associated with the relative spatial position of each individual aircraft with respect to its neighbor. This individual cost should reflect how well the operator is able to estimate the relative spatial positions between the two aircraft. In principle, an individual cost should be associated with each possible pair of aircraft in the area. This means that if the total number of aircraft is N, the number of individual pairs to consider is $0.5(N^2 - N)$. A preliminary course selection might reduce this number drastically, e.g. it will not be necessary to include the individual cost of pairs, of which the aircraft are far apart.

The optimization problem is defined as follows:

> *Find the viewing parameter setting, (2 translational parameters, i.e. the coordinates of the focus-of-interest in the ground plane, 2 rotational parameters, i.e. the azimuth and elevation angles of the viewing axis, and 1 ranging parameter), subject to the constraints set by magnitude of change limitations, which minimizes the global cost function J.*

5.4. Estimation of the Relative Spatial Position Between Aircraft

5.4.1. Geometry of the 3-D situation:

Fig. 11 shows the perspective view of two aircraft A and B, separated spatially, both in horizontal position and in height. The vector $\vec{R}_{AB}^{W}$, expressed in the World Coordinate System W, describes the position of aircraft B with respect to A. The length of this vector, $R_{AB} = \left\| \vec{R}_{AB}^{W} \right\|$, is the distance between the two aircraft. The projections of A and B

on the ground plane are A' and B'. The azimuth of B with respect to A is the angle Ψ_{AB} subtended between the line $A'B'$ and the axis x^W pointing to the north. The elevation of B with respect to A is the angle Θ_{AB} subtended between the line AB and the line AB'', parallel to the line $A'B'$ in the ground plane. Due to the perspective view, the angles Ψ_{AB} and Θ_{AB} appear distorted and are estimated usually larger or smaller than their actual value, as shown in Ref. 1, (see footnote, page 2). The errors in estimating the angles Ψ_{AB} and Θ_{AB}, as well as in estimating the range R_{AB}, are a function of the viewing parameters. Functional relations between these errors and the viewing parameters have been investigated experimentally and analytically in Ref. 1.

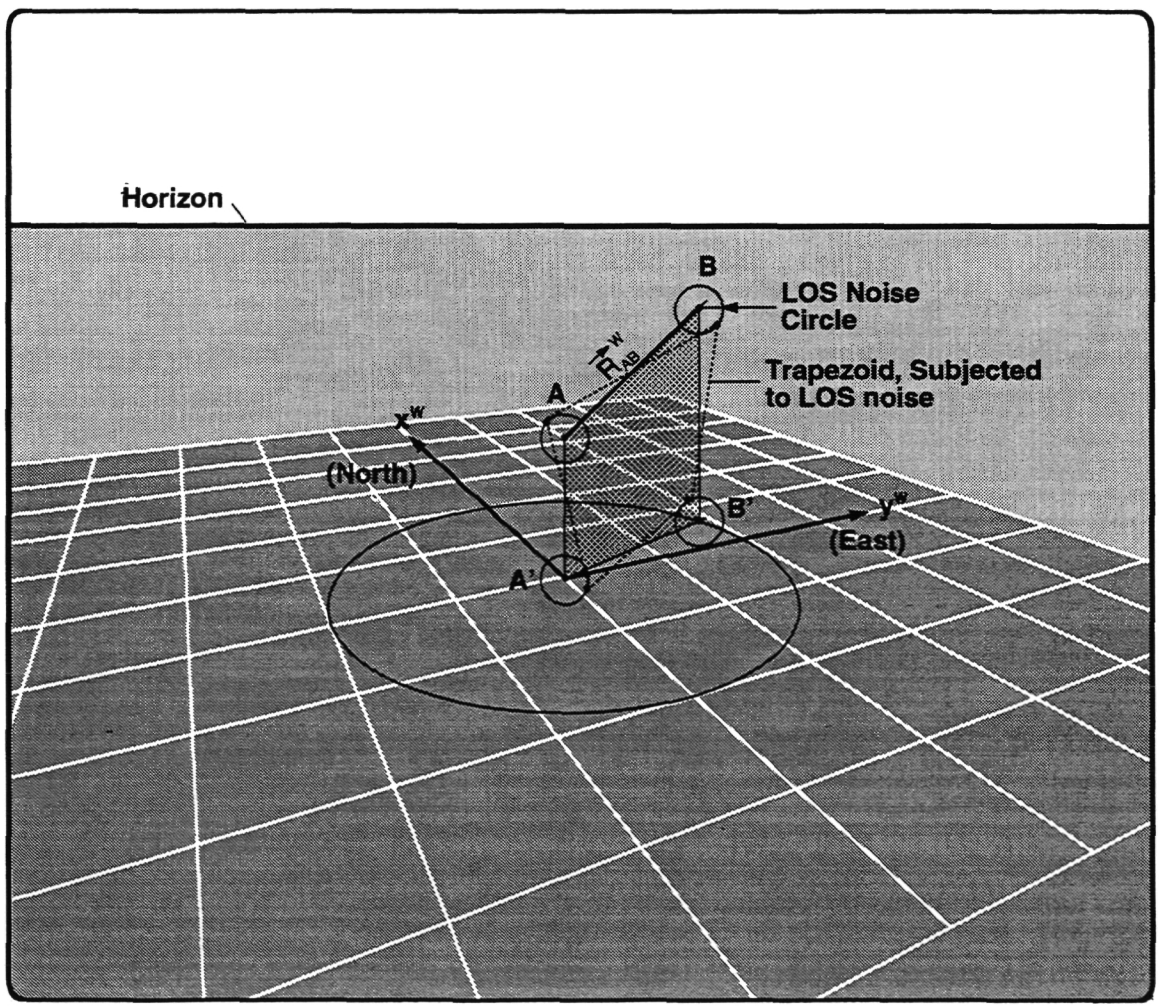

Figure 12.: The effect of line-of-sight noise on spatial estimates

It is clear that the angle Ψ_{AB} is best estimated, when the scene is viewed straight from above, i.e. a plan view. However, in that case the angle Θ_{AB} can not be estimated, i.e. the error in estimating Θ_{AB} becomes infinitely large. On the other hand, Θ_{AB} is best estimated when the observer's eye is located in the ground plane and the viewing axis is perpendicular to the plane $ABB'A'$, but then the error in estimating Ψ_{AB} might become very large.

5.4.2. Cost associated with estimation errors:

A cost can be associated with the errors in estimating the angles Ψ_{AB} and Θ_{AB}, and the range R_{AB}. This cost should reflect the expected error in the estimation of these variables. Thus, the cost should grow when the estimation errors are expected to be large.

Rather than associating a cost with the errors in estimating the angles Ψ_{AB} and Θ_{AB}, it might be more meaningful to an Air Traffic Control situation to associate a cost with the errors in estimating the vector $\vec{R}_{AB}^{W}$. The components of $\vec{R}_{AB}^{W}$ are given by:

$$\vec{R}_{AB}^{W} = \vec{x}_{B}^{W} - \vec{x}_{A}^{W} = \begin{bmatrix} x_{B}^{W} - x_{A}^{W} \\ y_{B}^{W} - y_{A}^{W} \\ z_{B}^{W} - z_{A}^{W} \end{bmatrix} \tag{13}$$

where $\vec{x}_{B}^{W}$ and $\vec{x}_{A}^{W}$ are vectors, describing the position of aircraft B and A in the W system. If the errors involved in estimating the vector $\vec{R}_{AB}^{W}$ are given by the error vector $\vec{\varepsilon}_{R}^{W} = \left\{ \varepsilon_{R_x}^{W} \quad \varepsilon_{R_y}^{W} \quad \varepsilon_{Rz}^{W} \right\}^{T}$, the cost, associated with the error in estimating the relative spatial orientation of aircraft pair AB could be formulated as:

$$J_{AB}^{2} = \frac{(\varepsilon_R)^2}{(R_{AB})^2} \tag{14}$$

where $\varepsilon_R = \left\| \vec{\varepsilon}_{R}^{W} \right\|$ denotes the length of the error vector. Note that Eq. (14) in fact expresses the 'noise-to-signal' ratio. For example, if this ratio is very large, it will be impossible to decide whether the aircraft are sufficiently separated from each other and the corresponding cost will become unacceptably high.

In Ref. 1, as mentioned in the footnote on page 2, a model for spatial orientation by familiarity cues has been developed and experimentally evaluated. This model is able to compute the error vector $\vec{\varepsilon}_{R}^{W}$ for each aircraft pair and viewing parameter setting. These computations are based on spatial, 3-D matching of the vertices of the trapezoid $ABB'A'$ to their corresponding perceived lines-of-sight. The model uses familiarity cues, based on a priori knowledge of the 3-D shape of the object, e.g. it utilizes the knowledge that the lines projecting on the ground plane, are parallel, that these lines are perpendicular to the ground plane, etc.

The model is based on the assumption that the inaccuracies, which exist in the perception of the lines-of-sight of the vertices of the trapezoid, are the main source of error in estimating the vector $\vec{R}_{AB}^{W}$. This is demonstrated in Fig. 12. The line-of-sight vector is corrupted by a noise vector of a constant magnitude, and located in a plane perpendicular to the line-of-sight. The in-plane angle, determining the orientation of this

noise vector, is distributed uniformly between zero and 360 degrees. The noise-corrupted line-of-sight vectors thus intersect the image plane at points located on the circles, centered at the trapezoid vertices. In the example of Fig. 12, the dotted, deformed trapezoid constitutes the input shape, on which the 3-D matching scheme is employed. Obviously, this deformed shape will lead to errors in the estimation of $\vec{R}_{AB}^{W}$. For each aircraft pair and each viewing parameter setting, the error vector $\vec{\varepsilon}_R^W$ is computed by a Monte Carlo method, in which the in-plane angles of the noise vectors are varied randomly. For a sufficiently large ensemble, the numerator of Eq. (14) will be the expected value: $E\left\{(\varepsilon_R)^2\right\}$, which is the power (or the second moment) of ε_R.

If the line-of-sight noise vector magnitude is considered to be constant, the error vector $\vec{\varepsilon}_R^W$, in principle, is a function of the 5 viewing parameters and the 6 parameters determining the trapezoid of the aircraft pair, i.e. 3 world coordinate components for each one of the aircraft.

In computing the power of ε_R, it is impractical to employ the spatial orientation model for each aircraft pair and a variety of viewing parameter settings in real time. However, the functional dependency of $\vec{\varepsilon}_R^W$ on all these parameters can be substantially simplified by realizing that the error vector $\vec{\varepsilon}_R^W$ mainly depends on the shape of the aircraft pair trapezoid on the image plane, as it appears to the operator. This appearance, in turn, will depend on the angular orientation of the trapezoid with respect to a reference line-of-sight to its center or to one of its corners. For convenience, this reference LOS is directed towards point A'. Thus, two parameters are needed for defining the angular orientation of the trapezoid $ABB'A'$ with respect to the line-of-sight to point A' [4]. Three additional parameters comprise the normalized dimensions of the trapezoid, i.e. the distances AA', BB' and AB, normalized with respect to the range measured along the line-of-sight to point A'.

A Monte-Carlo simulation in real-time on these 5 remaining parameters will still be too time-consuming, if a sufficiently large ensemble is to be generated. Fortunately, the experimental results of Ref. 1 have indicated, that the expected value of $(\varepsilon_R)^2$ can usually be modeled in terms of relatively simple trigonometric functions of the parameters determining the angular orientation of the trapezoid $ABB'A'$ with respect to the line-of-sight to point A'. The weighting coefficients, multiplying these trigonometric functions, depend on the shape of the trapezoid in 3-D space (not on the image plane), i.e. the normalized distances AA', BB' and AB. The spatial orientation model can be used to compute these weighting coefficients in real-time, and store them in a look-up table.

Thus, although the computation of $E\left\{(\varepsilon_R)^2\right\}$ by means of the model is complex and time-consuming, the use of trigonometric functions and retrieval of pre-computed data, might reduce this computation to a limited number of simple arithmetic operations, which might be easily realized in a real-time framework.

---

[4] These parameters will actually determine the shape of the trapezoid, as it will appear on the image plane. Note that the angular orientation is determined by two angles: a 'slant' angle and a 'twist' angle. This 'twist' about the line-of-sight to the point A', will have no effect on the apparent shape of the trapezoid on the image plane, and thus also not on the errors.

5.5. Computation of the Global Cost

The first part of the global cost, i.e. the cost J^1, being the cost relating to the area on the image plane at which the aircraft symbols appear, is computed as follows. Each point of the image plane surface is rated according to its distance from the central viewing area. The individual cost associated with aircraft A is given by:

$$J_A^1 = \frac{P_A}{r(x_s, y_s)} \tag{15}$$

where P_A is a value associated with the level of attention which should be given to the aircraft. For example, aircraft in danger of violating minimal separation distances, should be given a high level of attention.

The image plane surface rating $r(x_s, y_s)$ reflects the 'real estate' value of the screen location. It is necessary for realizing the optimization scheme, that this function should be continuous in the first derivative. Central locations are rated high and off-center locations are rated low. It should be noted that a small rating, different from zero, should be associated to areas *outside the* screen boundaries as well. This will assure that aircraft, demanding a high level of attention but outside the screen boundaries, will be moved into the visible range. The cost J^1 is computed by summing the individual costs given by Eq. (15), for all aircraft.

The second part of the global cost, i.e. the cost J^2, reflecting how well the operator is able to estimate the relative spatial positions between two aircraft, is the weighted sum of the costs associated with each one of the aircraft pairs, according to:

$$J^2 = \sum_j c_j J_j^2; \quad j = pair(A,B); pair(A,C); \cdots etc. \tag{16}$$

where the weighting factor c_j, by which each one of the individual costs is multiplied, is a function of the level of attention which should be given to the particular aircraft pair. For example, an aircraft pair which appears 'clustered' on the display, will have a high value of J_j^2. If also the required level of attention is high, i.e. c_j is large as well, the pair will have a high impact on the cost J^2, so that the optimization scheme will seek a solution which will attempt to 'de-cluster' the aircraft. However, if c_j is zero, i.e. it is not important that the operator is aware of the aircraft pair its relative orientation, the clustered aircraft pair will be ignored by the scheme.

5.6. Impact of Individual Aircraft on the Global Cost

It should be noted that although the global cost reflects a measure of the average performance of a large number of aircraft in the area, the optimization scheme will still be sensitive to display anomalies occurring with one single aircraft, or one single pair of aircraft.

For example, for aircraft outside the boundaries of the screen, the surface rating $r(x_s, y_s)$ in Eq. (15) will be very small and, provided P_A is non-zero (i.e. the aircraft should actually be visible), J_A^1 will be large and have a large impact on the global cost and the scheme will tend to move the aircraft within the boundaries of the screen.

Similarly, for an aircraft pair of which the vector $\vec{R}_{AB}^{W}$ can not be properly estimated, the error vector $\vec{\varepsilon}_{R}^{W}$ will be very large, and provided the weighting coefficient c_{AB} is non-zero (i.e., it is important that the operator is aware of aircraft pair AB its relative orientation), the term $c_{AB}J_{AB}^{2}$ will be large and have a significant impact on the global cost. In both cases the optimization scheme will seek a solution which will reduce the large individual costs, thus correcting display anomalies occurring with individual aircraft.

5.7. Optimization Method

Due to the complexity of the problem and the unconventional cost function, it is not yet sure whether conventional techniques such as the common numerical gradient method, limited search method, steepest descend method or a Newton-Raphson second-order scheme will be effective. Unconventional methods, e.g. *genetic algorithms for optimization* [5]will be attempted to solve the optimization problem. The robustness of the latter method, its ability to quickly reach optimal solutions for multimodal and discontinuous cost functions by searching from a population of starting points rather than one, and the fact that this methods does not require derivative or other auxiliary information, makes this technique a primary candidate for our complex optimization problem. The use of predetermined motion patterns might be necessary to limit the degrees-of-freedom and reduce the complexity of the search for a minimum. A design requirement is that the computations should be completed in a time-span which is one order-of-magnitude less than the time required to execute the viewing parameter change (through a slewing motion).

[5]Goldberg, D.E., "Genetic Algorithms in Search, Optimization, and Machine Learning," Addison-Wesley Publishing Company, Inc., Jan., 1989.

6

PROPOSED CONTINUED RESEARCH

6.1. Current Status of the Research

The MVPS system has been implemented in a generic framework for an Air Traffic Control display and incorporated into the CTAS perspective display at Ames Research Center. The software has been written for a Silicon Graphics, Indigo II system. It includes direct and indirect control over the viewing parameters by manipulation pointers, as outlined in Chapter 4. The changes are executed by appropriately tuned slewing functions. The parameters of the slewing functions can be adjusted at input level. The framework has the flexibility to include a large database of aircraft, terrain features and air-route maps and symbology.

The proposed planned activities will deal with the development of the AVPS system and its experimental evaluation. Since the ability of the operator to make accurate spatial judgments from the perspective scene plays an essential role in the optimization process underlying the AVPS system, part of the research efforts will be directed towards understanding the spatial reconstruction process in complex scenes. These efforts will include the development and experimental evaluation of enhanced noise models.

6.2. Analytical and System Developments

6.2.1. Enhanced visual perception modeling:

Although the visual perception model of Ref. 1 (footnote, page 2) yielded a close match between analytical and experimental results, its validity was tested for the relatively simple case of the two-body problem. The first body comprised the trapezoid formed by the two aircraft and their drop-lines, and the second body comprised the ground grid structure as shown in Fig. 12. The validity of the model in more complex situations is mainly determined by the model of the sources of inaccuracies. In the original model a relatively simple source of inaccuracy was introduced, i.e. LOS noise vectors of a constant-magnitude, determining 'circles of inaccuracy' with equal radii on the display, as seen in Fig. 12. This model assumes that the noise vectors of each one of the lines-of-sight are uncorrelated, independent from the perceived object shape, from the distance between neighboring objects and from the position of the object on the screen. Experimental validation results of the original model showed that the magnitude of the noise vectors was found to be at least one order-of-magnitude larger than the noise set by visual acuity or threshold considerations. This proves that the LOS noise does represent inaccuracies in the reconstruction process, rather than the inherent visual acuity inaccuracies at the 'front end'. The air traffic scene, with the complexity of a multiplicity of aircraft involved, will require enhancements of the noise model.

Figure 13.: Shape distortions for constant-magnitude and correlated LOS noise

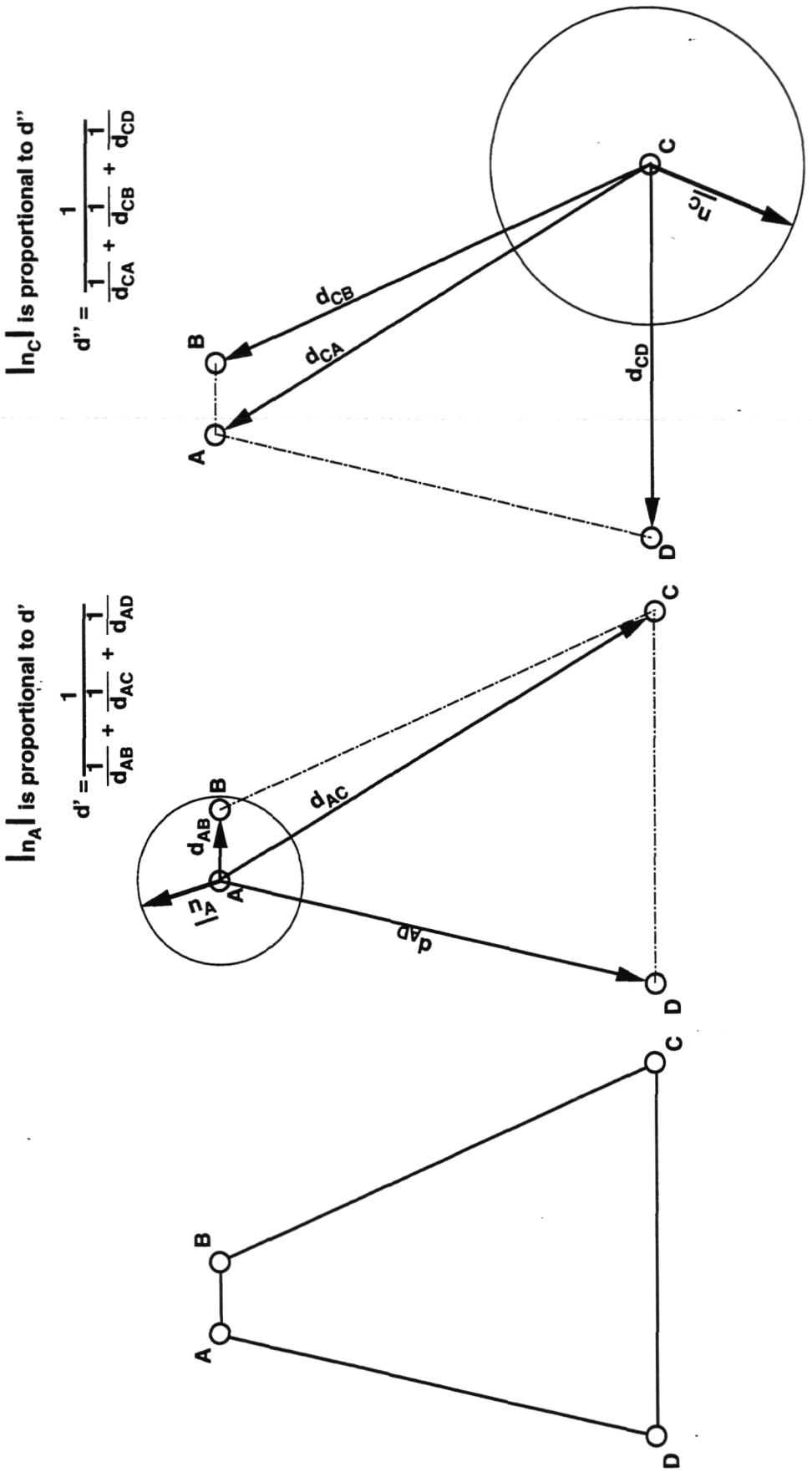

Figure 14.: LOS noise component, correlated with neighboring vertices

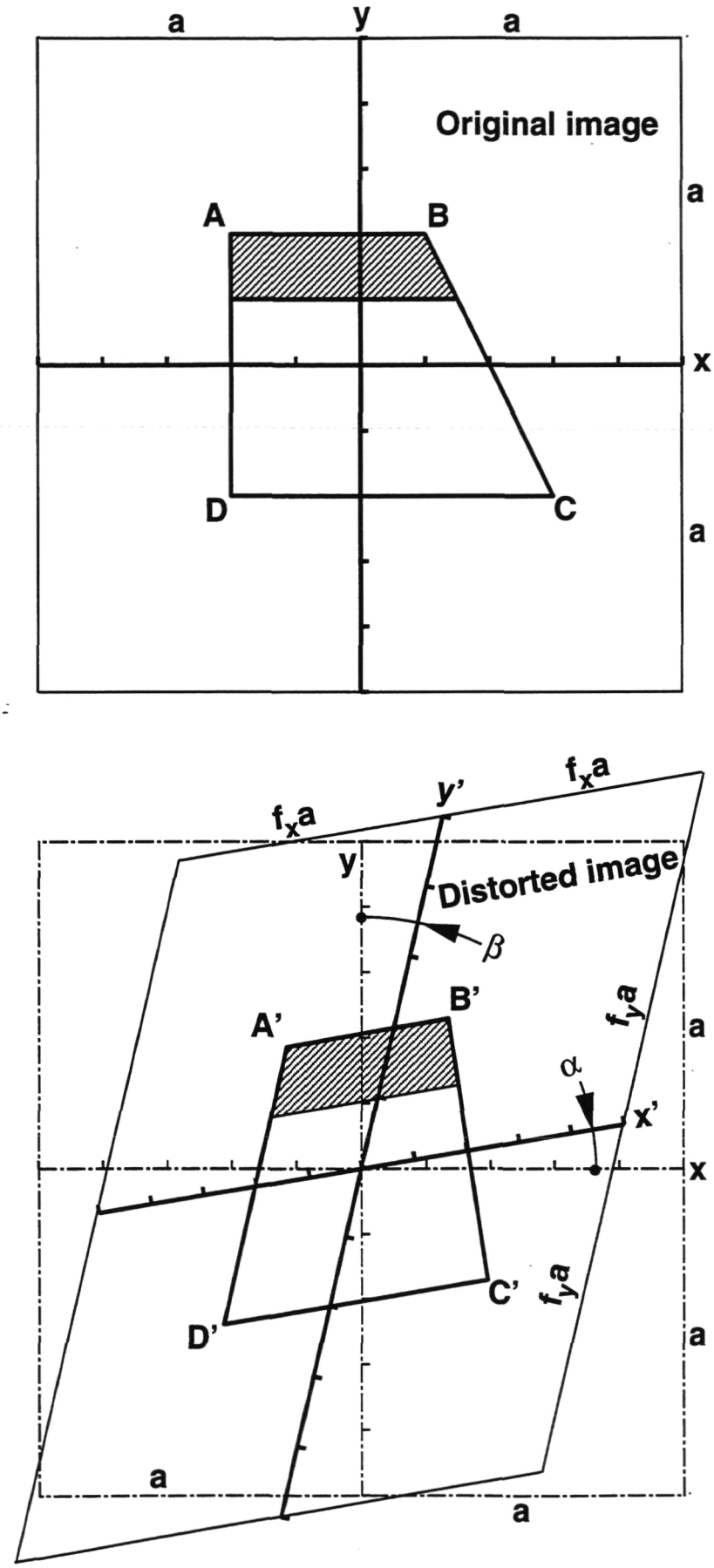

Figure 15.: Perceived object shape distortion

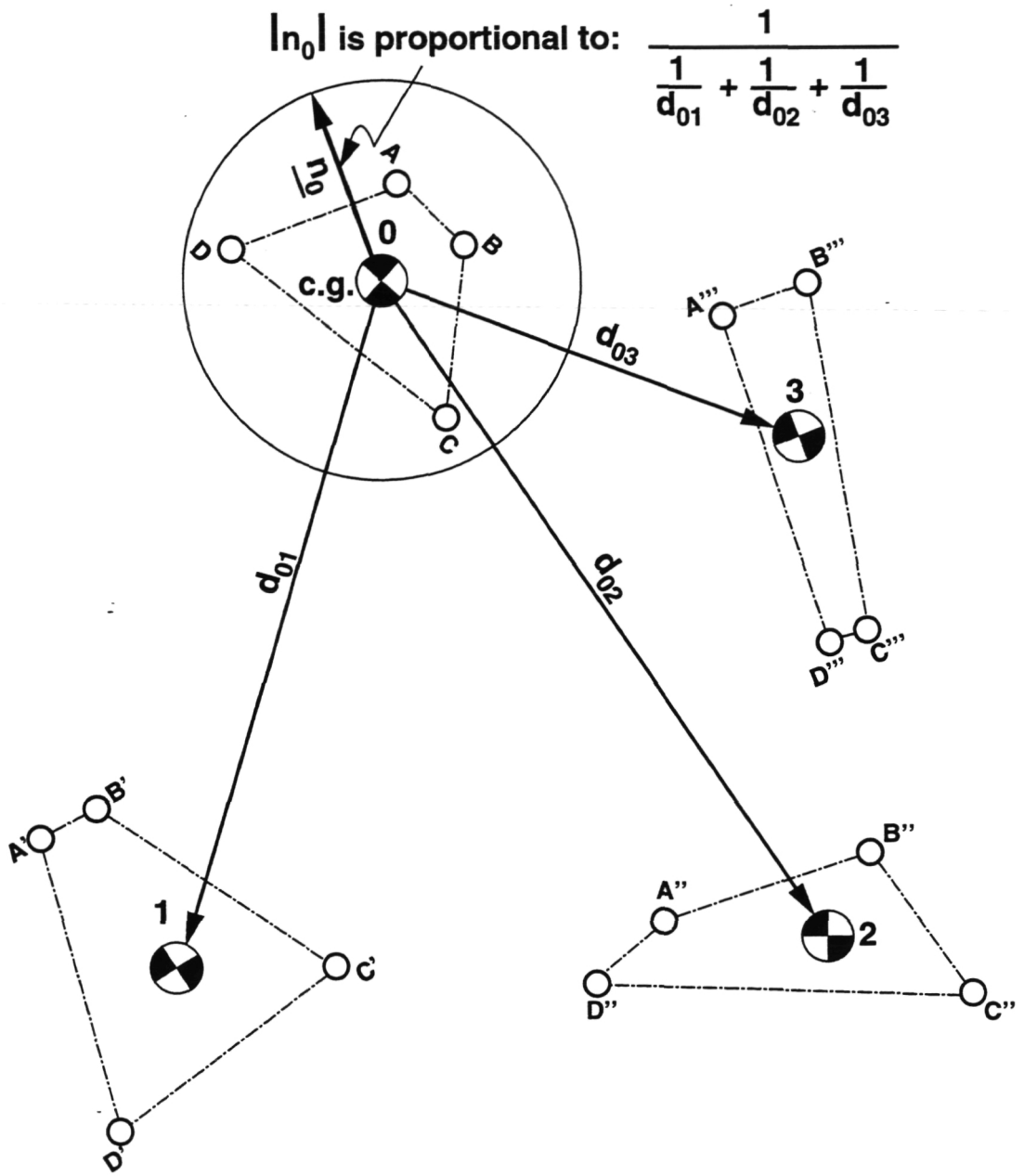

Figure 16.: Noise component, set by inter-object relations

The example in Fig. 13a demonstrates that the constant-magnitude LOS noise vector hypothesis might yield unacceptable results. The runway image, seen by the pilot of an aircraft on approach-to-landing as the trapezoid *ABCD*, is corrupted by constant-magnitude LOS noise. However, since the noise vectors do not consider the interrelation between the vertices, the shape will become unacceptably distorted. Moreover, the observer might perceive the trapezoid appearance of the runway quite accurately, but its relative position from the center of the screen or from other objects in the scene, might be perceived with a large degree of inaccuracy. In order to avoid these shortcomings, enhanced noise modeling is proposed.

6.2.2. Enhanced noise modeling for multi-object scenes:

The simple constant-magnitude noise model is not able to describe the complex multi-object interaction in the air-traffic scene. The proposed enhanced noise model accounts for the fact that the spatial reconstruction of the perspective scene is more accurate for objects of which the coordinates or shapes appear to be closely together on the image plane, than for objects of which the coordinates are further apart. This notion is well-known in instrument display tracking tasks, in which constant observation noise levels were found[6], i.e. the variance of the observation noise is proportional to the variance of the displayed signal. Therefore, the LOS noise of each one of the vertices is assumed to be composed of several components:

1. An *uncorrelated* baseline component; this component is identical to the constant-magnitude LOS noise component of the original model as seen in Fig. 12, with the difference that the magnitude is set by visual acuity considerations.

2. A noise component of which the magnitude is correlated with the distances to neighboring vertices. The reasoning behind this model is that it is more accurate to perceive the relative position between two neighboring vertices, when these vertices are located closely together on the image plane. Like in (1) the noise vector is situated in a plane perpendicular to the LOS and its direction is random, but the magnitude of the LOS noise of a particular vertex is a function of the harmonic mean of the distances to the neighboring vertices, see Fig. 14. The harmonic mean of the distances between vertex *A* and vertices *B*, *C* and *D* is given by:

$$d' = \frac{1}{\frac{1}{d_{AB}} + \frac{1}{d_{AC}} + \frac{1}{d_{AD}}} \tag{17}$$

   The harmonic mean is chosen as the representative distance to assure that in the presence of nearby neighboring vertices, the effect of far-away vertices is small. Hence, the magnitude of the distance-correlated LOS noise of point *A* is smaller than the one of point C, and the resulting distorted shape is shown in Fig. 13b.

3. A noise component, set by *perceived object shape considerations.* This component accounts for the fact that the observer also perceives the lines, interconnecting two vertices. Thus, lines that appear almost parallel, should be perceived as such. A general distortion, which preserves this property, is obtained by re-drawing the perceived shape in a distorted reference frame, of which the x-axis is rotated by the a.c.w. angle α and the y-axis by the c.w. angle β, and the axis scaling is changed by the factors f_x, and f_y, respectively. This distortion is shown in Fig. 15.

---

[6]Levison, W.H., Baron, S. and Kleinman, D.L. : "A Model for Human Conmtroller Remnant," IEEE Trans. on MMS, Vol. 10, No. 4, Dec. 1969, pp. 101-108.

The distorted perceived shape is obtained by the following transformation:

$$\begin{bmatrix} x \\ y \end{bmatrix}_{distorted} = \begin{bmatrix} \cos\alpha & \sin\beta \\ \sin\alpha & \cos\beta \end{bmatrix} \begin{bmatrix} f_x & 0 \\ 0 & f_y \end{bmatrix} \begin{bmatrix} x \\ y \end{bmatrix}_{undistorted} \tag{18}$$

The angles α and β and the scale factors f_x and f_y are random variables, with statistical properties which are identical for all perceived shapes in the scene.

4. A noise component, set by *inter-object* relations. This component accounts for inaccuracies in determining the relative orientation between the various object shapes. A 'center-of-gravity' of each one of the object shapes is computed. This center is perturbed by a noise vector of which the direction is random in a plane perpendicular to the LOS to the center-of-gravity, and the magnitude is computed in a manner similar to the correlated noise component of (2). Thus, for each center, this noise vector has a magnitude which is a function of the harmonic mean of the distances to the neighboring centers, as seen in Fig. 16.

5. A noise component accounting for inaccuracies in determining the *location* of the various object shapes on the screen. Although the various individual object shapes and the relations between them, might be perceived accurately, there might still be considerable inaccuracy in determining its location on the image plane. This inaccuracy is modeled by adding the *same* random noise component to all vertices in the screen. This is equivalent to randomly shifting the complete picture in horizontal and vertical direction. It is clear that this noise component will have its primary effect on the viewing direction angles.

6.2.3. Parametric study of the enhanced noise model:

A parametric study will be carried out to determine the effect of each one of the noise components on the spatial estimates. The air traffic scene can be considered as a multi-object problem, where the ground plane constitutes the first object, and the trapezoids, composed by two neighboring aircraft comprise the other objects. The spatial estimates of each one of the trapezoids and their inter-relation will contribute to a better estimate of the viewer's orientation with respect to the ground plane, and this improvement, in turn, will improve the estimates of the trapezoids.

From experience with the original two-object model it is known that errors in estimating the slant-angle of the viewing axis with respect to the ground-plane, are reflected almost directly in estimation errors in the dimensions of the aircraft-pair trapezoid. This means that although the objective of the observer's estimation process is to obtain accurate estimates of the vector $\vec{R}_{AB}^{W}$ for each one of the aircraft pairs, the quality at which the entire spatial lay-out can be reproduced is essential in reducing the estimation errors of $\vec{R}_{AB}^{W}$.

As mentioned in Section 5.4.2, the estimation of the spatial lay-out of the trapezoids, composed by two neighboring aircraft, involves 6 parameters, i.e. the three-dimensional world coordinates of each one of the aircraft. The spatial perception model will find estimates for the viewing parameters and the 6 trapezoid parameters for each one of the aircraft pairs, where the viewing parameters are: the viewing azimuth, the viewing elevation, the viewing range, the focus-of-interest x^w and y^w coordinates, and for an unknown station point, to some extent, the zoom angle.

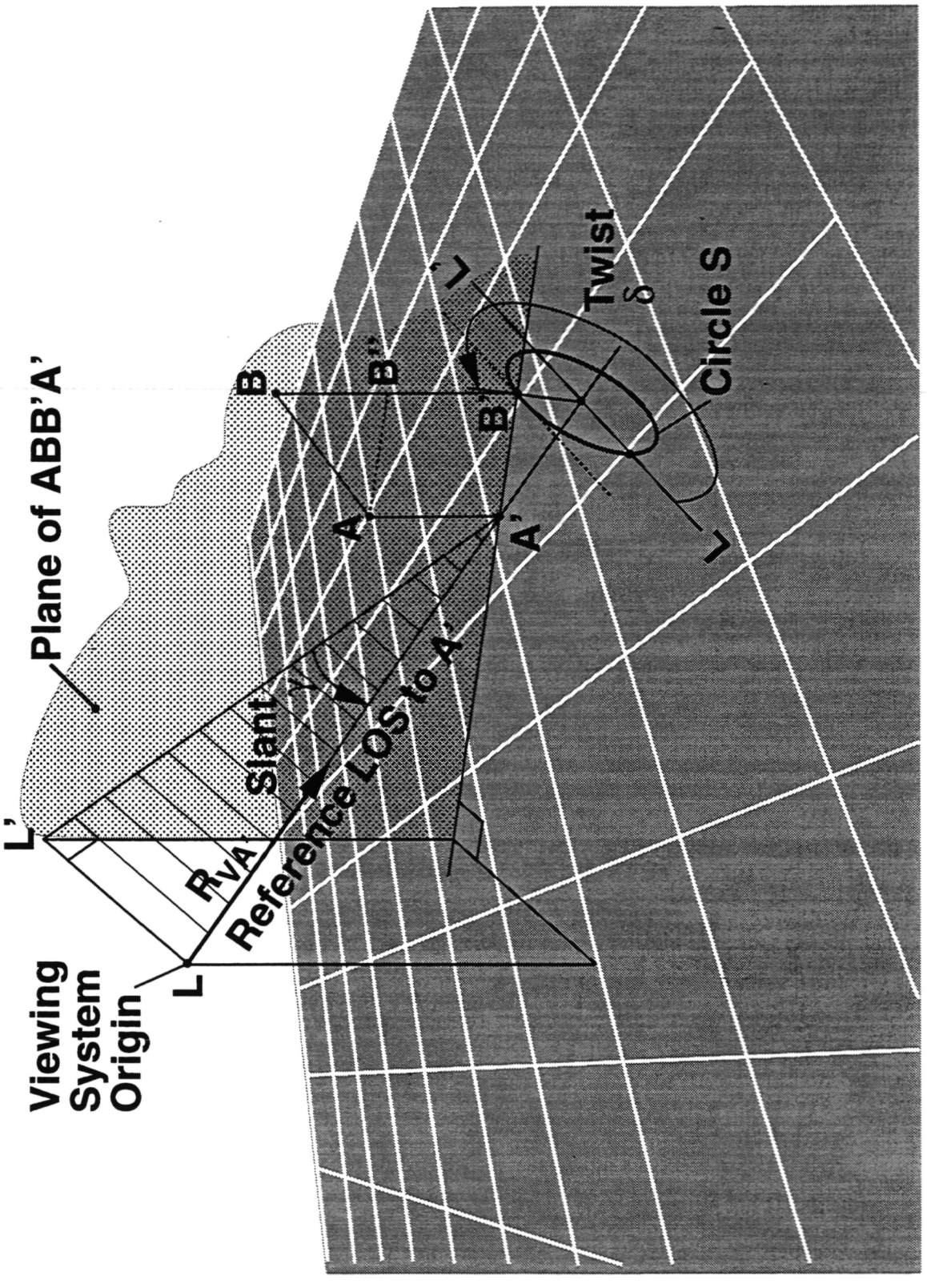

Figure 17.: Spatial orientation of trapezoid with respect to LOS to point *A'*

Rather then expressing the trapezoid in world-coordinates, it is more meaningful to the observer to express the spatial orientation of the trapezoid in terms of its angular orientation with respect to the reference LOS to the corner point A', and the range $R_{VA'}$ measured along the reference LOS to point A'. This spatial orientation determines the shape of the trapezoid as it appears to the operator on the image plane. The spatial situation is shown in Fig. 17.

The angular orientation is determined by two angles, a slant angle γ and a twist angle δ. The slant angle is the angle between the line VA', which is the LOS to point A', and the line $V'A'$, which is its projection on the trapezoid plane P. The twist angle determines the rotation of the trapezoid about the reference LOS. This rotation is determined as follows. Point B' is located on the circle S, centered at the reference LOS and located in a plane perpendicular to this LOS. The line LL' is a horizontal line through the center of the circle, i.e., the line LL'' is parallel to the groundplane. The twist angle δ is the angle, measured along the circle S, in positive LOS direction (for a right-hand system), between point L and point B'. The remaining 4 parameters are the trapezoid dimensions, AA' BB' *and* $A'B'$ and the range $R_{VA'}$.

The estimates of the spatial perception model, i.e. the viewing parameters and the 6 trapezoid parameters for each one of the aircraft pairs, can be expressed in terms of the slant and twist angles, and in terms of the 3 trapezoid dimensions, normalized with respect to the range $R_{VA'}$. The slant angle is expected to have its largest effect on the estimation errors of $\vec{R}_{AB}^{W}$, and the twist angle the smallest effect. The results of the parametric study will serve in composing analytical expressions or in compiling look-up tables for the expected value of $(\varepsilon_R)^2$. Input to these look-up tables would be the slant angle γ and the normalized distances AA', BB' and AB. These expressions or tables, in turn, will be utilized in the on-line AVPS optimization scheme.

6.2.4. AVPS system development:

These developments include the formulation of the cost functions, image plane surface rating function $r(x_s, y_s)$, level of attention function P_A, the expected value $E\{(\varepsilon_R)^2\}$ function, and the various weighting coefficients, to be used in the AVPS scheme. The aircraft database is to be included, and a sensitivity analysis is to be performed, in order to determine the sensitivity of the various cost function items to changes in viewing system parameters.

It is to be investigated in particular, whether and to which extent, cost function items are sensitive to typical perspective display singularities such as visual exclusions or ambiguities. Other tests include sensitivity of the cost function to changes in the level of required attention.

The results of this sensitivity analysis will determine the optimization scheme, which will be employed. The performance of the system will be tested in terms of its robustness to numerical instabilities, convergence to meaningful solutions, and its time required for one computation cycle. The use of predetermined motion patterns will be explored, in case complexity of the search for an optimum demands the reduction of the degrees-of-freedom or number of optimizable parameters.

6.2.5. Analytical tests of the AVPS system:

A wide range of analytical tests will be carried out to test the validity of the approach and to evaluate its performance. The ability of the AVPS system will be investigated in solving anomalies in the perspective representation, i.e. occlusions, ambiguities, etc. Furthermore, the response of the AVPS system to changes in the level of required attention will be investigated for a wide range of conditions.

6.2.6. Decision algorithm:

A decision algorithm will be developed that is to decide whether and when a change in viewing parameter setting should be initiated. The decision will be based on the current situation, the current viewing parameter setting, the computed optimal setting, and the time elapsed since the last change.

6.2.7. Path-planning algorithm:

A path-planning algorithm will be developed, which determines the spatial path as a function of time, along which the change in viewing parameters should be made. This algorithm will employ the 'slewing functions' for gradual, smooth transitions from one viewing parameter setting to another one, in order to ensure that the introduced changes will not negatively effect the spatial awareness of the operator.

Since a change in viewing parameters setting might involve a number of variables, path planning would involve coordination of the changes made in each one of the parameters as a function of time. Possible solutions are:

(1) Sequential changes: The changes are made sequentially, one parameter at the time. The parameter is varied from the initial setting to the final setting according to the slewing functions of section 3.2. The advantage of this method is that the resulting motions are easily understood and in-line with MVPS operations. A disadvantage of this method is that the total duration of the change will be longer, since it is composed of the sum of the times needed for the changes in each one of the individual parameters. An additional disadvantage is that the path might include viewing parameter settings which yield areas of the scene which are outside the visual field of the original setting. The resulting 'loss of correspondence' might negatively affect the spatial orientation. The sequence in which the changes are made, e.g. first translation, then rotation, then ranging, could be either fixed or adapted to the viewing situation.

(2) Simultaneous changes: the changes are made simultaneously, i.e. they take place in the same slewing time-span. The advantage of this method is that the change is made in the shortest possible time. The disadvantage is that the resulting motion patterns are complex and difficult to understand. Also here the path might result in a loss of correspondence between the initial and current setting.

(3) Complex path changes: at first a time-frame is set, in which the change should be completed. Next, a set of 'way points' along the path are defined. A way point is defined as a viewing parameter setting for a given point in time. The complex path has to pass through these way points. The way points should be chosen such as to prevent loss of correspondence. The actual path is determined by fitting a curve similar to the functions of section 3.2, through the way points. This method has the distinct advantage of allowing viewing parameter changes in the shortest-possible time, while preserving the correspondence between the initial and the current setting.

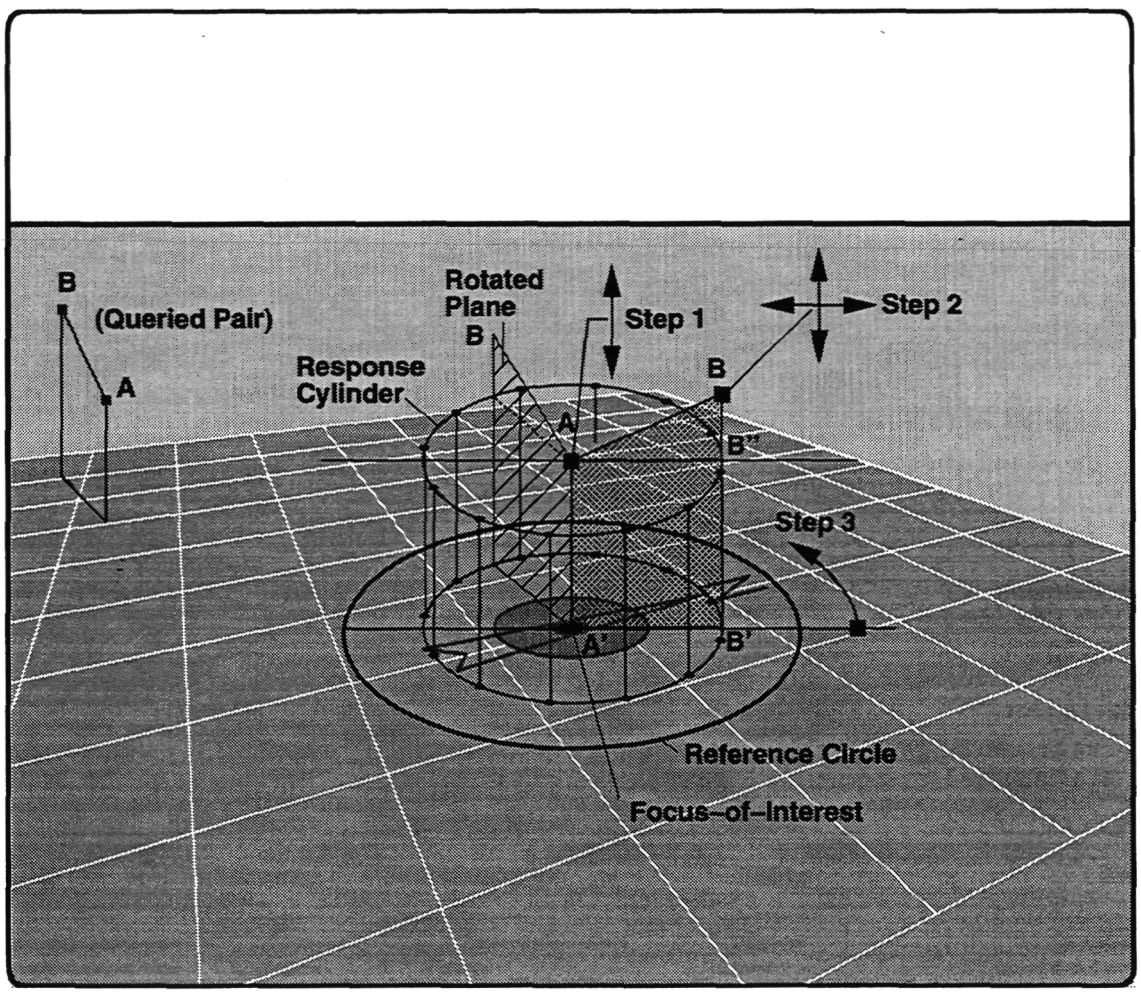

Figure 18.: Enhanced LOS noise model validation; the response trapezoid

6.3. Experimental Evaluations

6.3.1. Experimental validation of the enhanced noise model:

A limited series of qualitative experiments will be conducted to validate the enhanced multi-object noise model. A multi-aircraft scene will be presented for a given viewing parameter setting. While keeping this setting fixed, the observer is asked to draw a response trapezoid *AA'B'B* for a series of aircraft pairs (the queried aircraft pair will be highlighted on the display, where aircraft *A* will be highlighted first).

The response trapezoid is drawn in three steps. In steps 1 and 2 the trapezoid will be drawn as if it were viewed perpendicular and it will be of a size comparative to the ground plane reference circle, centered at the focus-of-interest, see Fig. 18. In step 3 the trapezoid will be rotated about a vertical axis to a direction which matches the estimated azimuth angle.

In steps 1 and 2 the response trapezoid is centered with point *A'* at the focus-of-interest and the line *A'B'* appearing horizontal on the image plane, i.e. parallel to the horizon. The observer shapes the response trapezoid by selecting and dragging points *A* and *B* with the mouse, in a manner similar to which this is done with the manipulation pointers. Point *A* can only be moved vertically (step 1), while point B can be moved both horizontally and vertically, (step 2). After the trapezoid has been shaped, step 3 takes effect, which involves setting the azimuth angle by selecting and rotating the base line *A'B'*. Note that the steps are executed sequentially without the ability to correct the settings of a previous step. Note also that the response cylinder will be drawn as well, see Fig. 18. The experiment is repeated for a variety of viewing parameter settings.

6.3.2. AVPS Operator-in-the-loop experiments:

A series of operator-in-the-loop experiments will be conducted to validate the system and to evaluate its effectiveness. These experiments will include abstracted, part-task experiments and full-task experiments.

(1) Part-task experiments : these experiments will concentrate on the ability of the operator to estimate spatial locations and orientations from the display. At first it will be investigated whether the viewing parameter setting suggested by the AVPS system, will yield smaller errors in the judgment of the relative positions between aircraft. This will be done by having the subject make the same judgments twice: once for a condition in which the global cost is high, and once when this cost has been brought to a minimum. In this experiment the subject will have no control over the viewing parameter setting, and 'static' viewing conditions will be used. (Note that slewing motions might improve spatial awareness, by adding motion cues). The same technique as described in paragraph 6.3.1 will be used. The conditions will be randomly accessed, have at least four repetitions, and the subject will be ignorant about the purpose of the experiment.

In a subsequent part-task experiment it will be investigated how *meaningful* the solutions of the AVPS system are to the operator. This will be done by repeating the previous experiment with the difference that the subject now has control over the viewing parameters by means of the MVPS system. The solutions of the AVPS system can be considered 'meaningful', when MVPS activity for situations with a low global cost, is much smaller than the one for situations with a high global cost. MVPS operations will include both direct as well as indirect control and the transitions will be performed by appropriate slewing motions. Note that the motion cues resulting from the slewing motions will improve the spatial awareness.

This experiment will be organized as follows. After the air traffic scene has been presented for a given viewing parameter setting, the operator has the option to change this setting, prior to starting the series of judgments on the individual aircraft pairs. Once this change has been completed, no further changes are possible until all judgments have been completed and until the next scene has been presented.

(2) Full-task experiments : these experiments will study the performance of the operator when the AVPS system is enabled or disabled. In both cases, the operator still has control over the viewing parameters through the MVPS system. Performance will be measured in terms of his abilities to carry out the controller's task, i.e. early detection of possible separation conflicts, spatial awareness, etc. Subjective ratings, like a 'handling qualities' scale, might be used as well.

6.3.3. Experimental evaluation of slewing functions:

The purpose of this series of experiments is to determine experimentally whether and to which extent, the gradual transitions from one viewing parameter setting to another through slewing functions, contribute to the spatial orientation. Furthermore, the best setting of slewing parameters for the various transitions, will be determined.

The experiments will include a spatial orientation task. A multi-aircraft air traffic scene will be shown. In this scene a number of randomly picked aircraft (a maximum of five) will be highlighted for a brief instant of time. The highlighting will be done sequentially, in a given sequence and in fixed intervals of time. The task involves to reproduce this sequence after the transition to the new viewing parameter setting has taken effect. However, the reproduction will take place a given fixed time-span after the sequence has been first presented. This time-span will be larger than the time needed for the longest-lasting gradual transition. The subject is asked to reproduce this sequence by successively selecting the aircraft with the mouse. Two experimental conditions will be considered: (1) gradual transitions employing the slewing functions, and (2) instantaneous transitions. Experimental parameters are: the magnitude and complexity of the change (more than one viewing parameter is changed) and the slewing parameters.

The comparison will be made with respect to a baseline test, in which the subject is requested to repeat a sequence after the same given fixed time-span as mentioned above, when no viewing parameter change has taken place. This test will also be used to determine whether the subjects have reached the required level of training. Production will commence, when reproduction errors will remain within preset bounds.

6.4. Summary of Proposed Activities Jan. 1, 1996 - Dec. 31, 1996

	Subject	Jan '96	Feb '96	Mar '96	Apr '96	May '96	Jun '96	Jul '96	Aug '96	Sep '96	Oct '96	Nov '96	Dec '96
1	Enhanced visual perception model development	✓	✓										
2	Enhanced noise model for multi-object scenes	✓	✓										
3	Parametric study of the enhanced noise model	✓	✓	✓									
4	AVPS system development		✓	✓	✓	✓							
5	Analytical tests of the AVPS system				✓	✓							
6	Decision algorithm				✓								
7	Path-planning algorithm				✓	✓							
8	Preparation of experiments	✓	✓	✓	✓	✓							
9	Experimental validation of the enhanced noise model				✓	✓			✓	✓			
10	AVPS Operator-in-the-loop experiments					✓	✓	✓	✓	✓	✓		
11	Experimental evaluation of slewing functions								✓	✓	✓		
12	Data processing, reporting										✓	✓	✓

Table 1.: Time table of proposed activities Jan. 1, 1996 - Dec. 31, 1996

Table 1 shows the planned activities and estimates for their duration. Activities 1-7 comprise analytical and system developments, and activities 9-11 include the experimental evaluation. Part of the experimental evaluation will be done at NASA/Ames during the principal investigator's stay at Ames, August-September, 1996. Preparation of all three experiments, activity 8, will be completed before the summer.

6.5. Estimated Budged for the Period Jan. 1, 1996 - Dec. 31 1996[7]

		Cost USD	Technion Cost Sharing
1.	**Salaries and Wages:**		
	Principal Investigator 1/3 time, 12 month	21,552	16,164
	Ph.D. Graduate Student 1/2 time for 12 month	19,440	19,440
	Programmer 1/4 time for 6 month	8,056	4,028
	Subtotal salaries and wages	49,048	39,632
	Overhead 25%	12,262	9,908
	Subtotal salaries and wages + overhead	61,310	49,540
2.	**Travel of Principal Investigator to NASA/Ames:**		
	Airfare 2 x $1,500	3,000	0
	Subsistence at Ames 75 days @ $110/day	8,250	0
	Subtotal travel expenses	11,250	0
3.	**Equipment Purchases:**		
	SGI Indy, 133 MHz, R4600PC	5,134	5,134
4.	**Materials and Services:**		
	Service contract for SGI equipment for 12 month	1,800	900
	Subjects (experiments) fee	800	450
	Subtotal material and services	2,600	1,350
6.	**Documentation:**		
	Printing, binding, photoshop, image processing	500	500
	Page charges	800	400
	Subtotal documentation	1,300	900
7.	**Miscellaneous:**		
	Postal charges, telephone calls	800	500
	Total cost of the project	**82,394**	**57,424**
	Technion cost sharing	**57,424**	
	Total budged requested from NASA	**24,970**	